Journal of the Iranian Chemical Society
https://doi.org/10.1007/s13738-021-02159-2

ORIGINAL PAPER

Synthesis, in vitro, and in silico studies of newly functionalized quinazolinone analogs for the identification of potent α-glucosidase inhibitors

Hayat Wali[1] · Ayaz Anwar[2] · Shahbaz Shamim[1] · Khalid Mohammed Khan[1,3] · Mohammad Mahdavi[4] · Uzma Salar[5] · Bagher Larijani[4] · Shahnaz Perveen[6] · Muhammad Taha[3] · Mohammad Ali Faramarzi[7]

Received: 20 September 2020 / Accepted: 2 January 2021

Abstract

Functionalized quinazolinone derivatives **1–30** were synthesized by two-step reaction. First, anthranilic acid was treated with substituted phenyl isothiocyanate to synthesize 3-aryl-2-thioxo-2,3-dihydroquinazolinone derivatives **1–8** which in turn reacted with different bromoacetophenone derivatives to obtain fully functionalized quinazolinone derivatives **9–30**. Both reactions were catalyzed by triethylamine. All the products were characterized by EI-, HREI-MS, ^{1}H-, and ^{13}CNMR spectroscopic techniques. All compounds were subjected to their in vitro α-glucosidase inhibitory activity. Results showed that except compound **1–3**, **5**, **7**, and **22**, all compounds were found potent and showed many folds increased α-glucosidase enzyme inhibition as compared to standard acarbose ($IC_{50} = 750.0 \pm 10.0$ μM). Compound **13** ($IC_{50} = 85.0 \pm 0.5$ μM) was recognized as the most potent analog of the whole series, with ninefold enhanced inhibitory potential than the standard acarbose. Compounds **1–9**, **11**, **12**, **22**, and **26** were structurally known compounds, while remaining all are new. Kinetic study on compound **13** showed that the compound is following a competitive-type inhibition mechanism. Furthermore, in silico studies have also been performed to better rationalize the interactions between synthetic compound and active site of the enzyme.

Supplementary Information The online version contains supplementary material available at https://doi.org/10.1007/s13738-021-02159-2.

✉ Khalid Mohammed Khan
khalid.khan@iccs.edu; drkhalidhej@gmail.com

[1] H. E. J. Research Institute of Chemistry, International Center for Chemical and Biological Sciences, University of Karachi, Karachi 75270, Pakistan

[2] Department of Biological Sciences, School of Science and Technology, Sunway University, Subang Jaya, 47500 Selangor, Malaysia

[3] Department of Clinical Pharmacy, Institute for Research and Medical Consultations (IRMC), Imam Abdulrahman Bin Faisal University, P.O. Box 1982, Dammam 31441, Saudi Arabia

[4] Endocrinology and Metabolism Research Institute, Tehran University of Medical Sciences, Tehran, Iran

[5] Dr. Panjwani Center for Molecular Medicine and Drug Research, International Center for Chemical and Biological Sciences, University of Karachi, Karachi 75270, Pakistan

[6] PCSIR Laboratories Complex, Karachi, Shahrah-e-Dr. Salimuzzaman Siddiqui, Karachi 75280, Pakistan

[7] Department of Pharmaceutical Biotechnology, Faculty of Pharmacy, Tehran University of Medical Sciences, Tehran, Iran

Published online: 20 January 2021

Graphic abstract

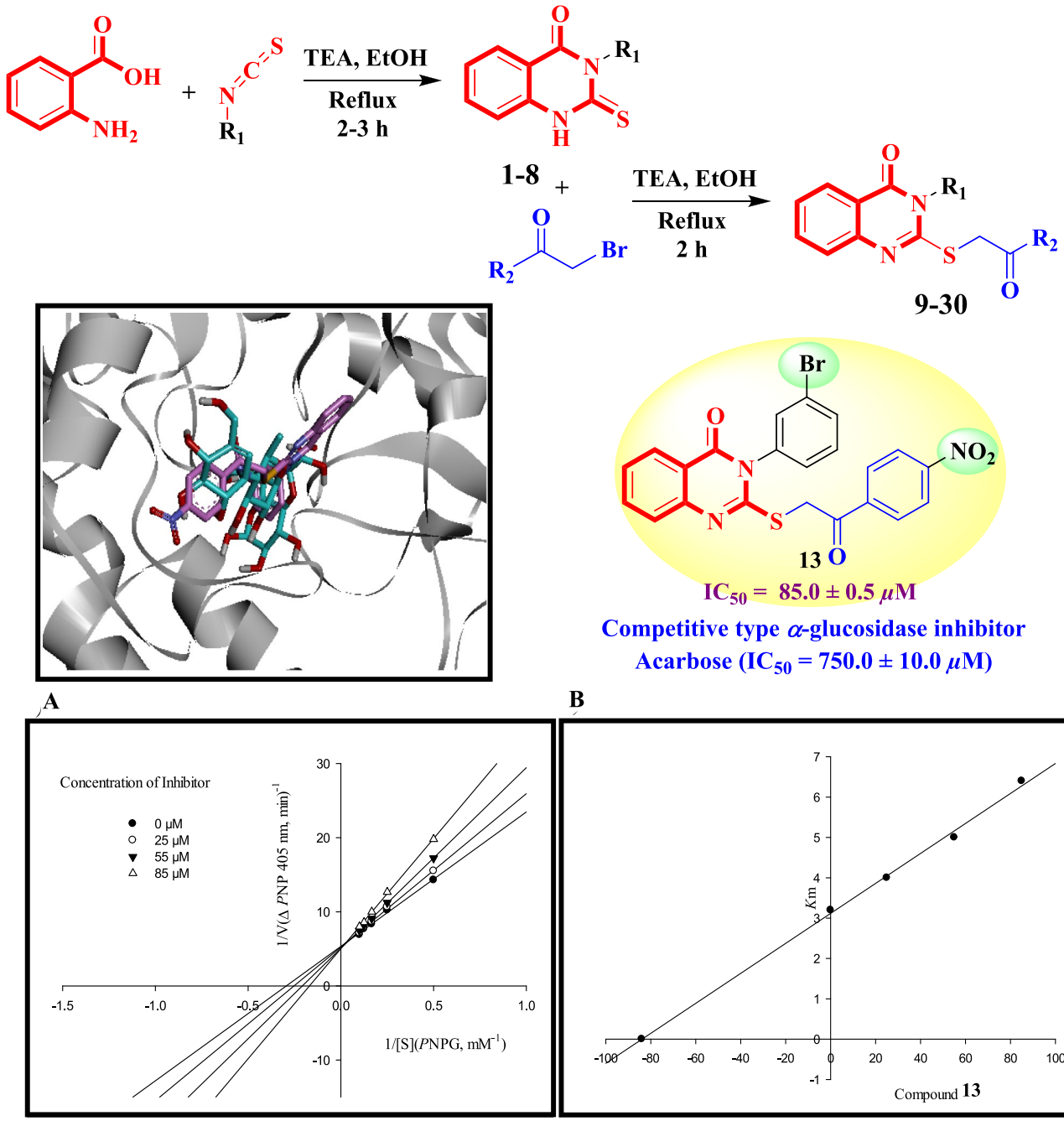

Keywords Quinazolinone · Synthesis · α-Glucosidase · Diabetes mellitus type II · In vitro · Kinetics · In silico

Introduction

Diabetes is the 6th leading cause of global mortality, and the most recent WHO (2018) report suggests that over 4.22 billion world population have been affected from diabetes. Diabetes is an ailment of carbohydrate, fat, and protein metabolism with multiple etiologies, resulting from failure in insulin secretion (type I diabetes), insulin dysfunction (type II diabetes), or both [1–5]. Type II diabetes accounts for about 80–90% of all cases of diabetes, and it is a widespread, chronic, multifactor, and metabolic disorder [1, 6]. α-Glucosidase and α-amylase are hydrolases, well known to

degrade polysaccharides such as starch, maltose, and sucrose into simple monosaccharides. α-Glucosidase (EC3.2.1.20) enzyme is a glycosyl hydrolase-31 located in small intestinal cells. It hydrolyzes 1,4 α-glycosidic bond of oligosaccharides and generates α-D glucose which is absorbable into the blood stream through the intestinal walls. [7]. There are two proposed mechanisms for hydrolysis: One is nucleophilic displacement, and the second is oxocarbenium ion intermediate [8]. Hyperactivity of α-glucosidase leads the rapid conversion of carbohydrates into glucose molecules which get absorb in blood stream and ultimately lead to postprandial hyperglycemia [9]. Post-prandial hyperglycemia is primary indication for type II diabetes mellitus [10, 11]. Conversion of carbohydrate into glucose can be suspended by inhibition of α-glucosidase enzyme which is one of the therapeutic ways to control and manage type II diabetes [12–14]. Some classes of compounds such as sulfonylureas, biguanides (metformin), meglitinides, and thiazolidinediones are used as oral drugs to treat type II diabetes but associated with several side effects [15, 16]. Utilizing commercially available therapies, only 36% of type II diabetes mellitus patients achieve glycemic control [17]. Therefore, new treatments for this chronic disorder are desperately needed [18] which can utilize safely and effectively to treat this disease.

Quinazolinone scaffold and their derivatives are pharmacologically important and dynamic group of molecules. Different positions of carbonyl group on quinazolinone result in two structural isomeric forms [19]. Quinazolinone alkaloid was first isolated from the Chinese plant *aseru* [20]. One of the first synthesized quinazolinone was methaqualone which was initially used as antimalarial drug, and later, it was used against insomnia [21]. A more satisfactory synthetic scheme was developed by Gabriel in 1903 [22]. The pharmacological importance of quinazolinone alkaloids those are isolated from microorganisms, animals, plants, as well as having synthetic origins is well documented [23–25]. Quinazolinone derivatives have a range of bioactivities such as anticancer, sedative, antihyperlipidemic, antihypertensive, and antiviral [22, 23, 26–28]. They have identified as dihydrofolate reductase (DHFR) [28, 29] and phosphodiesterase (PDEs) inhibitors [30]. The main pharmacophoric groups in quinazolinone compounds are carbonyl group at position 4, nitrogen atom at position 1, π system as well as their relative distances [31]. Many of the biologically active quinazolinones have substitution of oxygen or sulfur at C-2 [23].

In the near past, biological assessment of quinazolinones has gained huge interest and proven promise with the discovery of potent anticancer, antiviral, and antiparasitic agents [32–34]. Since many years, our research team is engaged in identification of several classes of heterocyclic compounds including 1,4 dihydropyridine, indazole, quinazolinone, benzotriazole, and coumarin as potential leads to α-glucosidase inhibitory activity [35–42]. We discovered 2-arylquinazolin-4(3*H*)-ones as new class of α-glucosidase inhibitors [39]. In this scenario, we urged to further explore this class for their α-glucosidase inhibitory potential (Fig. 1). For that purpose, we synthesized fully functionalized quinazolinone moieties by substituting ring nitrogen as well as sulfur with aryl and different phenacyl rings in order to evaluate their α-glucosidase inhibitory activity through in vitro and in silico studies.

Results and discussion

Chemistry

A series of functionalized quinazolinones **1**–**30** were synthesized by two-step reaction scheme. In the first step, anthranilic acid was treated with substituted phenyl isothiocyanate in the presence of catalyst trimethylamine (TEA) in ethanol to 3-aryl substituted quinazolinones **1**–**8**. Then, 3-aryl substituted quinazolinones **1**–**8** were reacted with different bromoacetophenone derivatives in ethanol. Again trimethylamine (TEA) was used as catalyst to obtain the desired quinazolinone derivatives **9**–**30** (Scheme 1). Reaction progress was checked by TLC analysis (ethyl acetate/hexanes, 3:7 for **1**–**8** and 100% DCM for **9**–**30**). Formation of the expected products (**1**–**30**) was confirmed by EI-MS, HREI-MS, ^{1}H- and ^{13}C-NMR spectroscopic techniques. Compounds **1**–**8**, **9**, **11**, **12**, **22**, and **26** were structurally reported [43–45], while rest of the derivatives are new.

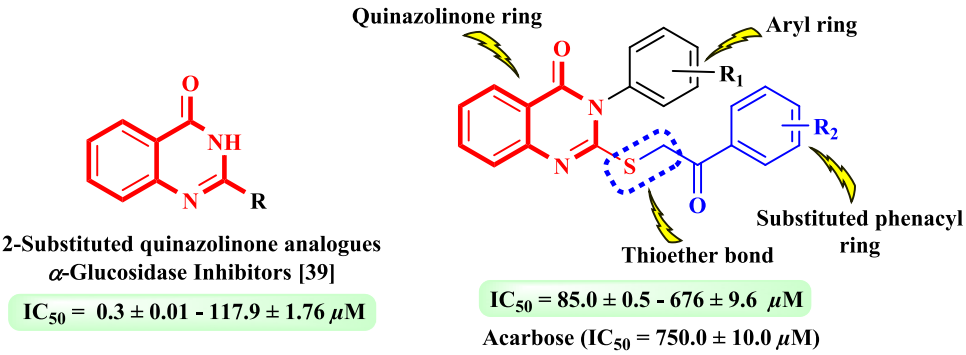

Fig. 1 Rationale behind the study

Scheme 1 General synthetic strategy for the synthesis of compounds **1**–**8** and **9**–**30**

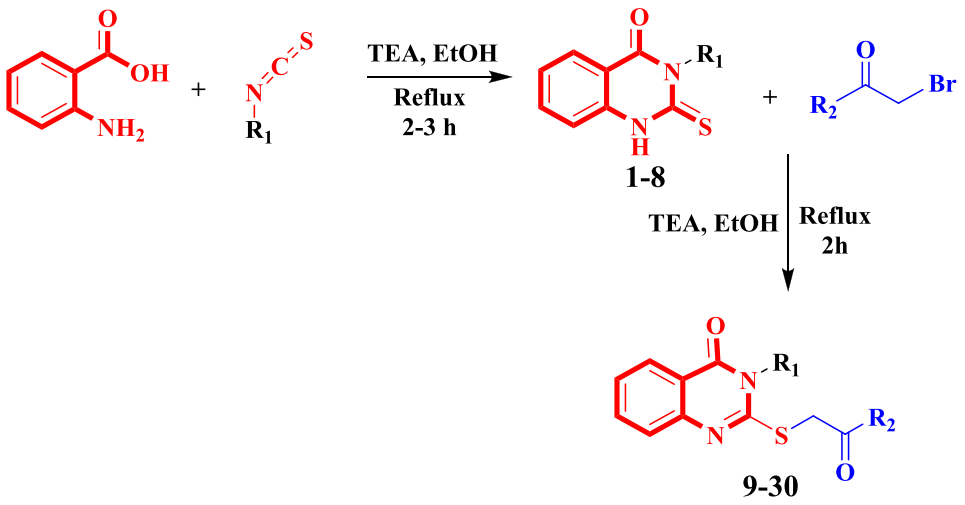

In vitro *α*-glucosidase inhibitory activity

All synthetic compounds **1**–**30** were subjected to in vitro *α*-glucosidase inhibitory activity. Results in terms of IC_{50} values showed that except compounds **1**–**3**, **5**, **7**, and **22**, all analogs ($IC_{50} = 85.0 \pm 0.5$–676.2 ± 9.6 µM) were found potent when compared to standard acarbose ($IC_{50} = 750.0 \pm 10.0$ µM). Interestingly, analog **13** ($IC_{50} = 85.0 \pm 0.5$ µM) was recognized as ninefold more potent than standard acarbose (Table 1).

Structure–activity relationship (SAR)

All synthetic quinazolinones **1**–**30** showed varying degree of inhibitory potential against *α*-glucosidase enzyme which could be defensible based on variations in substitution pattern on phenyl rings, electronic and steric factors. Thus, for simplifying SAR, compounds were divided in two categories "**A**" and "**B**." Compounds **1**–**8** are included in category "**A**," while remaining compounds **9**–**30** are listed as category "**B**."

Category "**A**" comprised of intermediates **1**–**8** showing significant to weak inhibitory potential in the range of IC_{50} values of 191.1 ± 2.5–377.2 ± 4.2 µM. Among these intermediates, compounds **4** ($IC_{50} = 312.4 \pm 3.2$ µM), **6** ($IC_{50} = 191.1 \pm 2.5$ µM), and **8** ($IC_{50} = 377.2 \pm 4.2$ µM) showed potent inhibitory potential as compared to the standard acarbose ($IC_{50} = 750.0 \pm 10.0$ µM), while remaining were found to be inactive with IC_{50} values greater than 750 µM. Unsubstituted compound **1** was found to be weakly active, while most potent intermediate **6** possesses *p*-nitro substitution at aryl ring which shows that nitro substitution is playing vital role in the inhibitory potential. Switching the nitro from *para* to *meta* makes the compound **5** inactive. This inactivity suggests that *para* position is more favorable for nitro group to actively participates in the *α*-glucosidase inhibition which might be by making important interactions with the active site of enzyme. However, replacing the *p*-nitro with *p*-ethoxy as in case of compound **4** slightly decreases the inhibitory activity which gives a perception that groups at *para* position might interact effectively with the active site of enzyme as compared to the other positions. In contrast to *para* substituted compounds **4**, **6**, and *p*-methoxy substituted analog **3** was found to be inactive. Compounds **2** and **7** having *o*-methoxy and *o*-fluoro were also found to be inactive (Fig. 2).

Fully functionalized compounds **9**–**30** with substituted aryl (**b**) and benzoyl (**c**) rings belong to category "**B**." In this category, except compound **22**, all compounds displayed potent *α*-glucosidase inhibitory activity ($IC_{50} = 85.0 \pm 0.5$–676.2 ± 9.6 µM). It is important to note the *p*-nitro substitution was present on benzoyl ring of compounds **10**–**19**. Among these analogs, compound **13** ($IC_{50} = 85.0 \pm 0.5$ µM) bearing *m*-bromo substituted aryl ring showed ninefold enhanced inhibitory activity as compared to the standard acarbose. This analog was also recognized as the most potent analog of the whole library. It seems that *m*-bromo group along with *p*-nitro substitution is playing a crucial role in the inhibitory activity. The second most active compound **18** ($IC_{50} = 90.7 \pm 0.6$ µM) having *p*-nitro group on aryl ring showed eightfold more potency than the standard. Comparison of its activity with its precursor/intermediate **6** ($IC_{50} = 191.1 \pm 2.5$ µM) revealed that incorporation of *p*-nitro-substituted benzoyl ring brought twofold enhanced inhibitory potential. Switching the position of nitro from *para* to *meta* on aryl ring in case of compound **19** ($IC_{50} = 100.0 \pm 0.9$ µM) exhibited a slight decreased activity. Nevertheless, the compounds were recognized as multi-folds potent than its inactive precursor **5**. Similarly, switching the position of nitro from *para* to *meta* on benzoyl ring leads to a sharp decline in the activity, as observed in the case of analog **20** ($IC_{50} = 163.2 \pm 1.7$ µM). Seemingly, *para* position

Table 1 In vitro α-glucosidase inhibitory activity of quinazolinone analogs 1–30

Comp.	R_1	IC_{50} ± SEM[a] (μM)	Comp.	R_1	IC_{50} ± SEM[a] (μM)
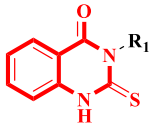 Category "A"					
1	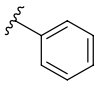	NA[b]	5	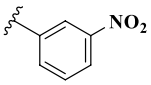	NA[b]
2	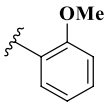	NA[b]	6	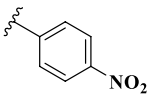	191.1 ± 2.5
3	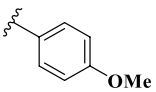	NA[b]	7	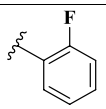	NA[b]
4	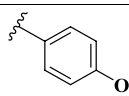	312.4 ± 3.2	8	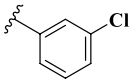	377.2 ± 4.2
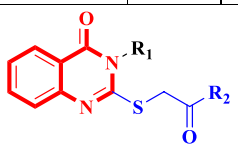 Category "B"					

Comp.	R_1	R_2	IC_{50} ± SEM[a] (μM)
9	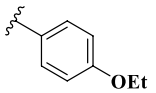		167.0 ± 1.8
10	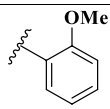	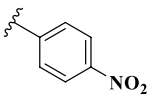	307.0 ± 3.2
11	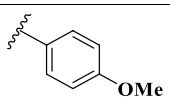	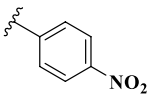	183.5 ± 2.1
12	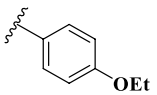	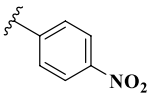	143.2 ± 1.2
13	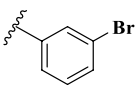	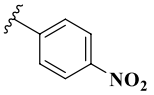	85.0 ± 0.5
14	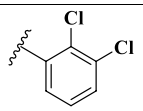	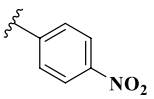	186.7 ± 2.2
15	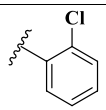	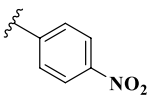	231.1 ± 3.5
16	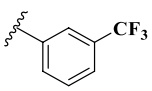	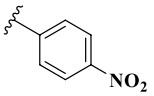	232.5 ± 3.5

Table 1 (continued)

17	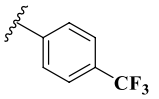	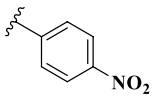	305.6 ± 3.1
18	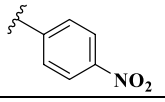	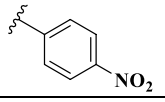	90.7 ± 0.6
19	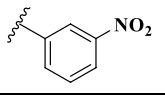	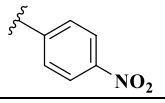	100.0 ± 0.9
20	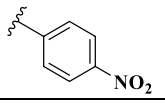	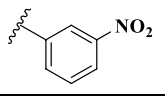	163.2 ± 1.7
21	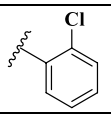	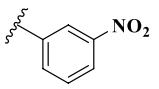	676.2 ± 9.6
22	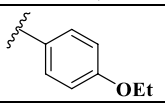	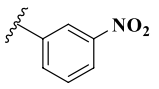	750 <
23	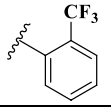	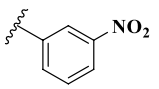	219.6 ± 2.9
24	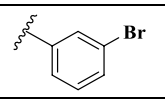	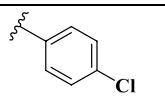	338.7 ± 3.6
25	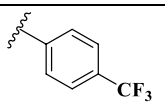	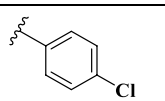	142.1 ± 1.2
26	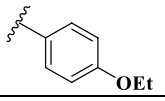	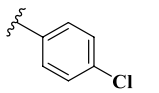	150.6 ± 1.4
27	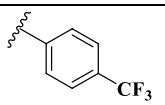	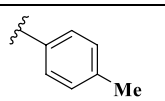	344.5 ± 3.7
28	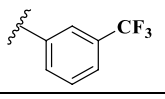	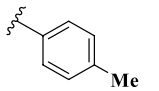	176.4 ± 1.9
29	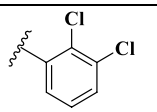	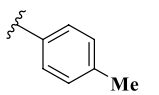	605.3 ± 9.1
30	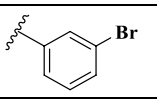	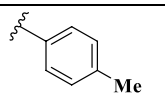	172.4 ± 1.9
Standard = Acarbose[c]			750.0 ± 10.0

[a] *SEM* standard error mean

[b] *NA* not active

[c] *Acarbose* standard inhibitor of α-glucosidase enzyme

nitro substitution interacts with the active site at its best. Activity of compound **13** can be compared with analog **16** ($IC_{50} = 232.5 \pm 3.5$ μM) which has trifluoromethyl substitution at aryl ring instead of bromo, and almost threefold decreased activity was observed. Switching the position of trifluoromethyl from *meta* to *para* further lowered the inhibition strength as observed in case of compound **17** ($IC_{50} = 305.6 \pm 3.1$ μM). In contrast to that switching, the position of trifluoromethyl from *meta* to *ortho* and nitro (on benzoyl ring) from *para* to *meta* in compound **23**

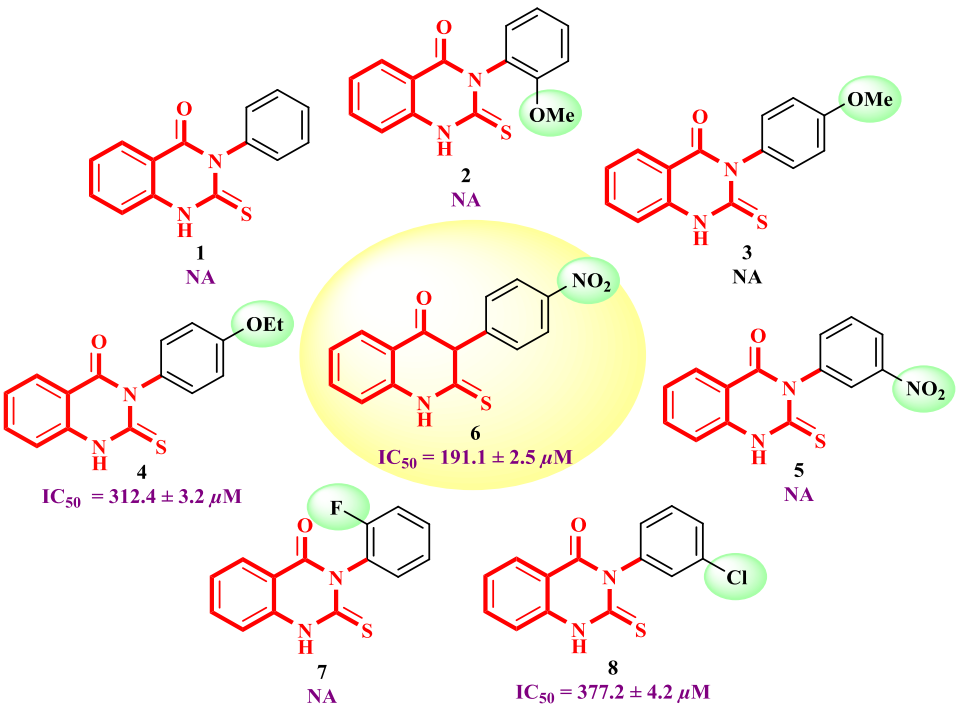

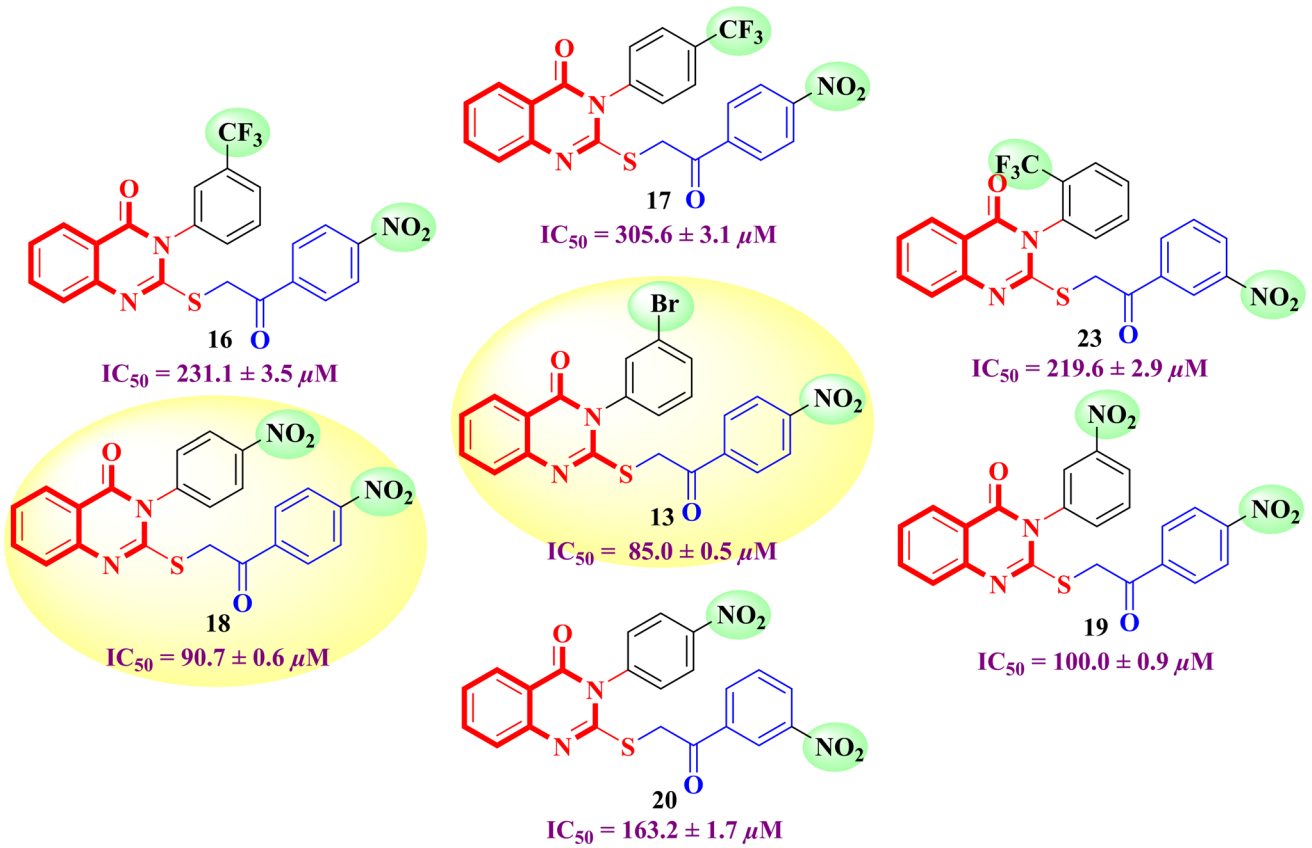

Fig. 2 α-Glucosidase inhibitory activity comparison of compounds **1**–**8**

Fig. 3 α-Glucosidase inhibitory activity comparison of compounds **13**, **16**–**20**, and **23**

(IC_{50} = 219.6 ± 2.9 µM) increased the inhibitory potential (Fig. 3).

Another compound **12** (IC_{50} = 143.2 ± 1.2 µM) is distinctively similar to second most potent compound **18** but has *p*-ethoxy instead of *p*-nitro on aryl ring and showed less inhibitory strength. This comparison affirms that ethoxy is less susceptible than nitro group particularly at *para* position, to interact with the active site of enzyme. Switching the nitro group from *para* to *meta* in compound **22** (IC_{50} = 750 < µM) also brought a sharp decline in the inhibitory strength. Activity comparison of compounds **12** with **11** (IC_{50} = 183.5 ± 2.1 µM) revealed that *p*-ethoxy is comparatively better than *p*-methoxy substitution which might be due to good electron donating ability which increases the electron density on aryl ring, so that it can better interact with enzyme. Switching the methoxy from *para* to *ortho* further lowers the inhibitory strength, as observed in case of compound **10** (IC_{50} = 307.0 ± 3.2 µM) which gives a perception that methoxy at *ortho* position is not interacted better than *para* position. Inhibitory activity of analog **10** can be compared with compound **15** (IC_{50} = 232.5 ± 3.5 µM) having *o*-chloro instead of *o*-methoxy, showing increased potential. Interestingly, addition of another chloro at *meta* position of aryl ring of compound **14** (IC_{50} = 186.7 ± 2.2 µM) further lifted up the inhibitory strength. However, moving the nitro substitution on benzoyl ring from *para* to *meta* in case of compound **21** (IC_{50} = 676.2 ± 9.6 µM) brought a sharp decline in the inhibitory strength (Fig. 4).

Compound **25** (IC_{50} = 163.2 ± 1.7 µM) bearing *p*-chloro and *p*-trifluoromethyl on benzoyl and aryl rings, respectively, was found to be fivefold more potent than the standard acarbose. Replacing *p*-trifluoromethyl with *p*-ethoxy on aryl ring in case of compound **26** (IC_{50} = 150.6 ± 1.4 µM) gives a slight decline in the inhibitory potential, while replacing the *p*-chloro with *p*-methyl on benzoyl ring in compound **27** (IC_{50} = 344.5 ± 3.7 µM) leads a decline in the inhibitory potential which gives a perception that electron-withdrawing groups at *para* positions of aryl and benzoyl rings stimulates the inhibitory strength. Moreover, activity comparison of compounds **25** with **24** (IC_{50} = 338.7 ± 3.6 µM) revealed that replacement of *p*-trifluoromethyl with *m*-bromo brought more than twofold decline in the inhibitory strength.

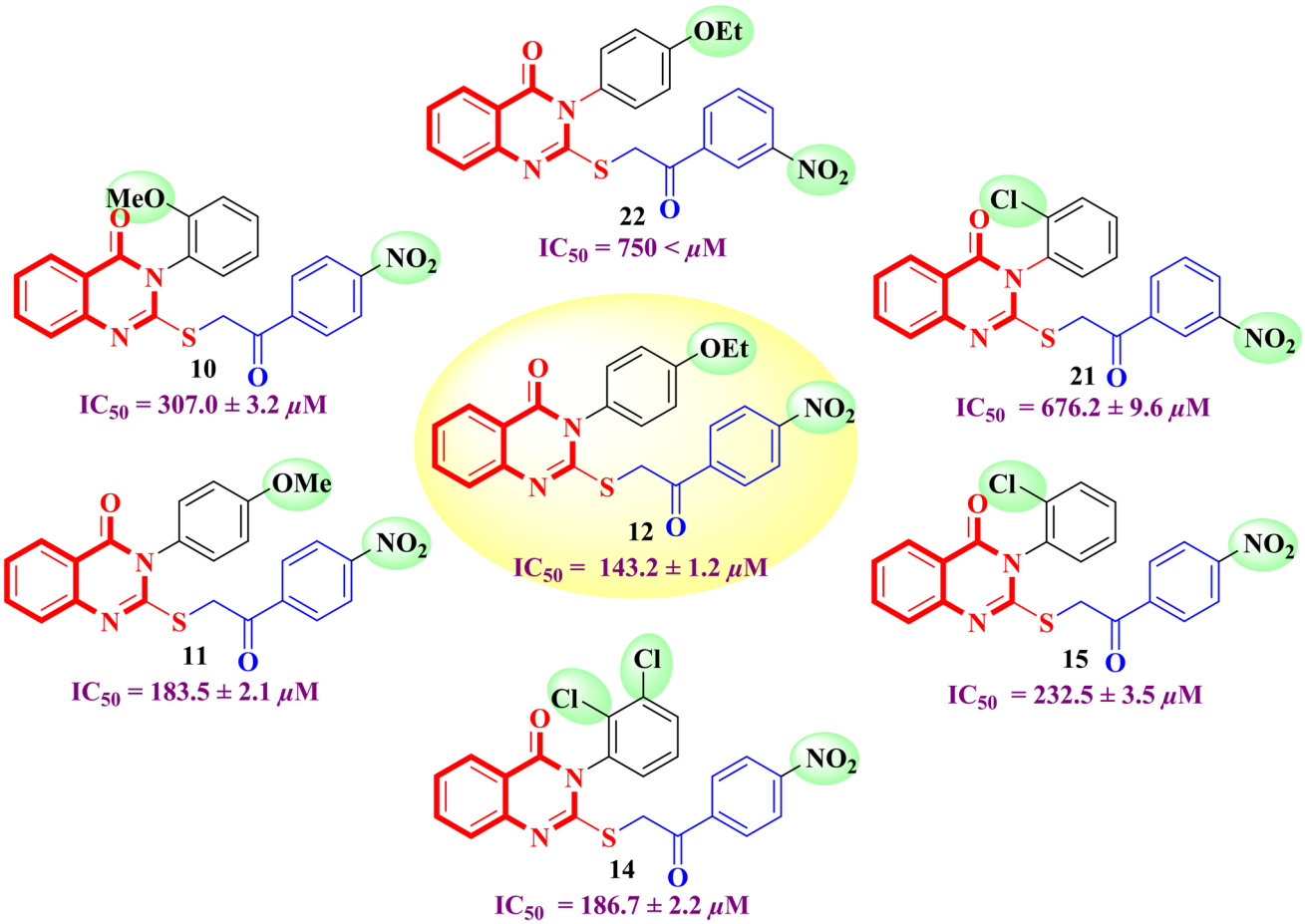

Fig. 4 *α*-Glucosidase inhibitory activity comparison of compounds **10**–**12**, **14**, **15**, **21**, and **22**

Similarly, activity of compound **24** can be compared with compound **30** ($IC_{50} = 172.4 \pm 1.9$ µM) which has *p*-methyl instead of *p*-chloro on benzoyl ring and showed doubled inhibitory potential. Replacing *m*-bromo with *m*-trifluoromethyl on aryl ring in compound **28** ($IC_{50} = 176.4 \pm 1.9$ µM) demonstrated almost same inhibitory strength. Incorporation of *o*,*m*-dichloro groups on aryl ring in compound **29** ($IC_{50} = 605.3 \pm 9.1$ µM) showed threefold less inhibitory activity as compared to compounds **28** and **30**. One exception was found in compound **9** ($IC_{50} = 167.0 \pm 1.8$ µM) which has ethyl acetate instead of benzoyl ring and displayed potent inhibitory strength comparable to many potent analogs. Its good activity might be due to hydrogen bond accepting property of ester group which may play a crucial role in the inhibitory strength (Fig. 5).

In brief, limited SAR suggests that almost all substitutional variations including electronic factor, size, and position of substitutions on aryl and benzoyl rings are playing vital role in the determination of inhibitory activity. However, electron-withdrawing nitro and bromine groups favors the inhibitory strength of compounds especially when present at *para* and *meta* positions, respectively. Switching the position of nitro group on aryl and benzoyl rings causes slight decrease in inhibitory activity. However, still all compounds were found to be many folds better inhibitors of α-glucosidase enzyme as compared to the standard acarbose. In order to predict the mode of inhibition, kinetic studies were conducted, while to rationalize the binding interactions of the potent compounds with the active site, in silico study was conducted.

Kinetic study of α-glucosidase enzyme inhibition

Compound **13** with lowest IC_{50} value is the most active, and its inhibition mode against α-glucosidase activity was analyzed with changed concentrations of substrate (*p*-nitrophenyl α-D-glucopyranoside) (2–10 mM) in the absence and presence of compound **13** at different concentrations 0, 25, 55, and 85 µM. To find out the type of inhibition, a Lineweaver–Burk plot was generated and the value of Michaelis–Menten constant K_m was deduced from plot between reciprocal of the substrate concentration 1/(*S*) and reciprocal of enzyme rate 1/*V* over different inhibitor concentrations. Experimental inhibitor constant K_i value was raised by secondary plots of the inhibitor concentration *I* versus K_m.

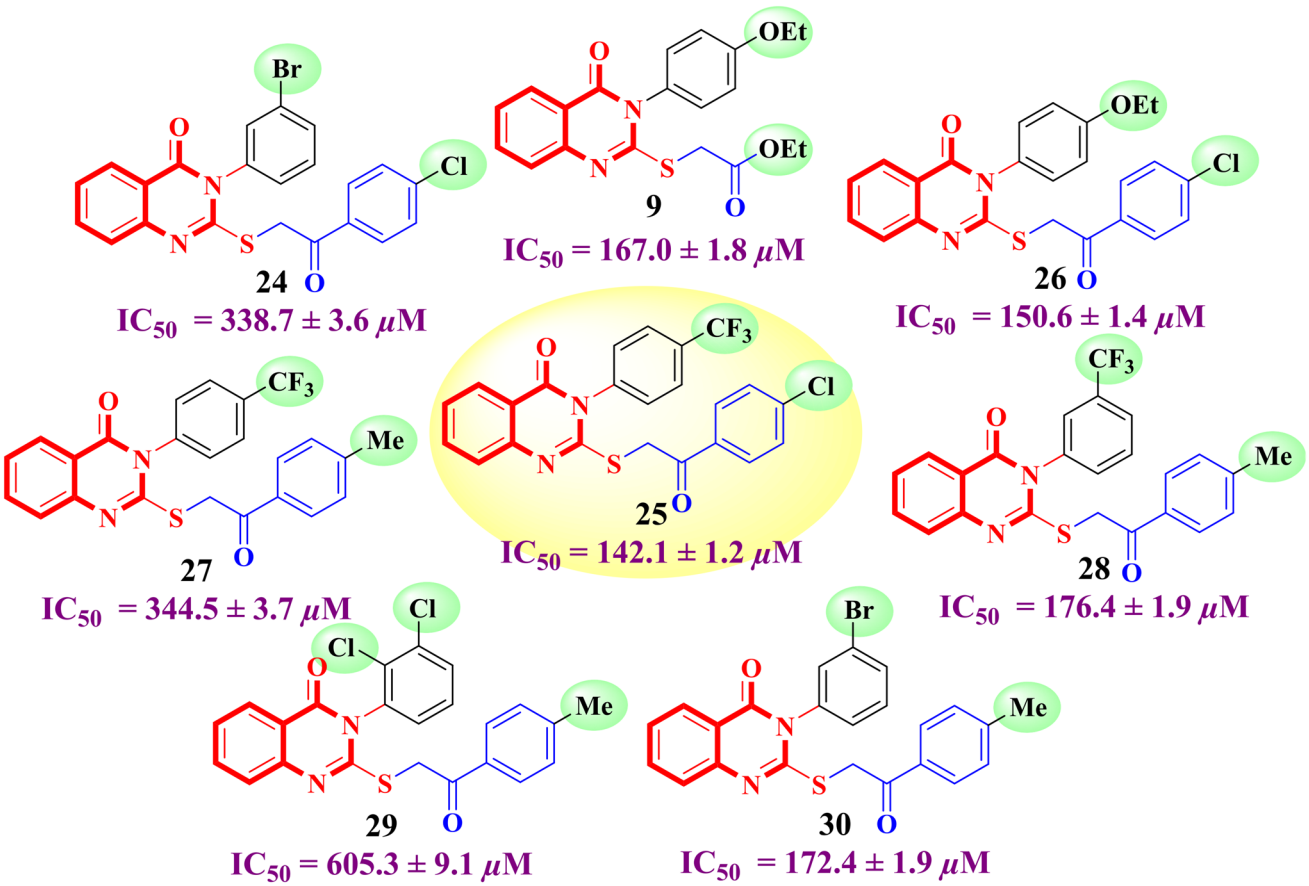

Fig. 5 α-Glucosidase inhibitory activity comparison of compounds **9** and **24–30**

According to Fig. 6a, the Line Weaver–Burk plot showed that the K_m gradually increased, and V_{max} remained unchanged with increasing inhibitor concentration indicating a competitive inhibition. The results show compound **13** bind to active site on the enzyme and compete with the substrate for binding to the active site. Furthermore, plot of the K_m versus different concentrations of inhibitor gave an estimate of the inhibition constant, K_i of 84 µM (Fig. 6b).

Docking study

To evaluate the interaction modes, binding energies, and amino acid interactions of the most active compounds, docking study was performed into modeled α-glucosidase using Auto Dock Tools (version 1.5.6) [43–46]. 3D structure of the standard inhibitor acarbose is shown in Fig. 7a. Superimposed of the most potent compound **13** on acarbose revealed that this new compound fitted well in the active site (Fig. 7b). The detailed interaction mode of acarbose revealed that this inhibitor interacted with active site residues Gln322,

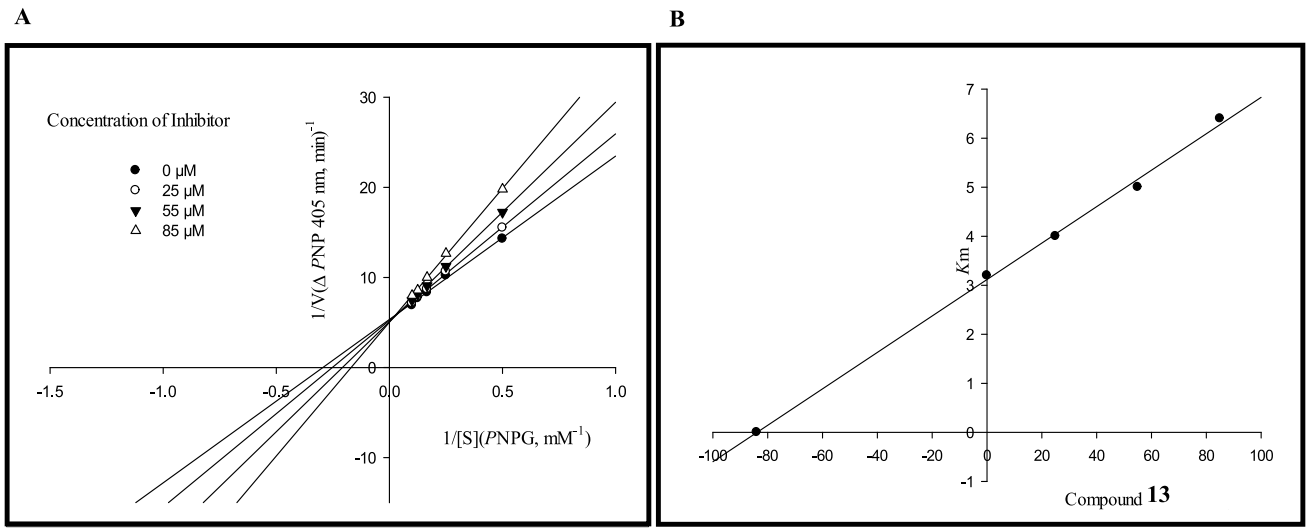

Fig. 6 Kinetic analysis of α-glucosidase inhibition by compound **13**. **a** Lineweaver–Burk plot in the absence and presence of different concentrations of compound **13**. **b** The secondary plot between K_m and various concentrations of compound **13**

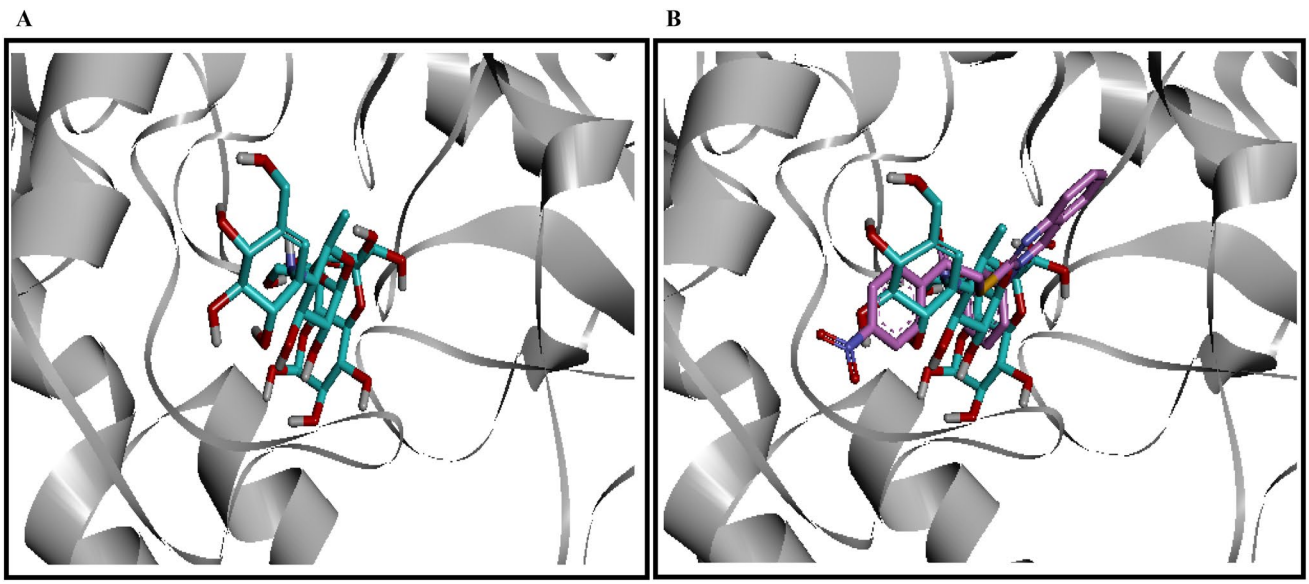

Fig. 7 **a** Acarbose in the active site of modeled α-glucosidase. b Acarbose (cyan) and the most potent compound **13** (pink) superimposed in the modeled α-glucosidase active site pocket

Thr301, His279, Arg312, Thr307, Glu304, Ser308, and Asn241 (Fig. 8a). The value of the binding free energy of acarbose is − 4.04 kcal/mol. Interaction mode of the most potent compound **13** is shown in Fig. 8b. It can be seen quinazolinone ring formed a π-cation and a π–π interactions with His279 and a hydrogen bond with Asn241. 3-Bromophenyl ring attached to quinazolinone core interacted with Glu304 via a π-anion interaction and Arg312 via a hydrophobic interaction. Furthermore, phenyl ring of 4-nitrophenyl moiety interacted with Val305 through a hydrophobic interaction.

Calculation of the binding energy of compound **13** (− 8.11 kcal/mol) predicted that this compound attached to active site easily than the standard drug. Quinazolinone ring of the second most potent compound **18** established a hydrogen bond with Gln322 and two hydrophobic interactions with Val305 and Pro309 (Fig. 9a). 4-Nitrophenyl ring attached to 3-position of quinazolinone ring formed a hydrophobic linkage with Thr301. Other 4-nitrophenyl ring of compound **18** interacted with Glu304 and Arg312 through a π-anion interaction and a hydrophobic interaction, respectively. Furthermore, this compound formed van der Waals interaction with Gly306, His279, His239, and Phe311. Binding energy of this compound was − 7.83 kcal/mol. Removing group attached to sulfur of compound **18**, as in compound **6** led to a moderate decrease in the inhibitory activity.

It can be seen in Fig. 9b, compound **6** established a hydrogen bond, a π–anion interaction, and two hydrophobic interactions with active site residues Thr307, Glu304, and Pro309 through quinazolinone core. 4-Nitrophenyl ring attached to this core formed a hydrogen bond and a π–π interaction with His239 via nitro group and phenyl ring and a π-cation interaction with His279 via phenyl ring. Binding energies of compounds **18** and **6** were − 7.83 and − 6.49 kcal/mol.

Conclusion

Thirty functionalized quinazolinone derivatives were synthesized and investigated for their α-glucosidase inhibitory potential by in vitro, kinetics, and in silico studies. Compound **13** along with many other analogs was identified as most potent analogs of the series. Limited SAR suggested that along with many structural features, electron-withdrawing nitro and bromine groups favor the inhibitory potential especially when present at *para* and *meta* positions. Kinetic study of compound **13** has been carried out to determine the type of enzyme inhibition. Lineweaver–Burk plot showed that the K_m gradually increased, and V_{max} remained unchanged with increasing inhibitor concentration indicating a competitive inhibition. In silico studies revealed a number of indispensable interactions between compound and active site of the α-glucosidase enzyme. This study has recognized a number of potent molecules that may serve as leads to future research in the identification of antidiabetic agents.

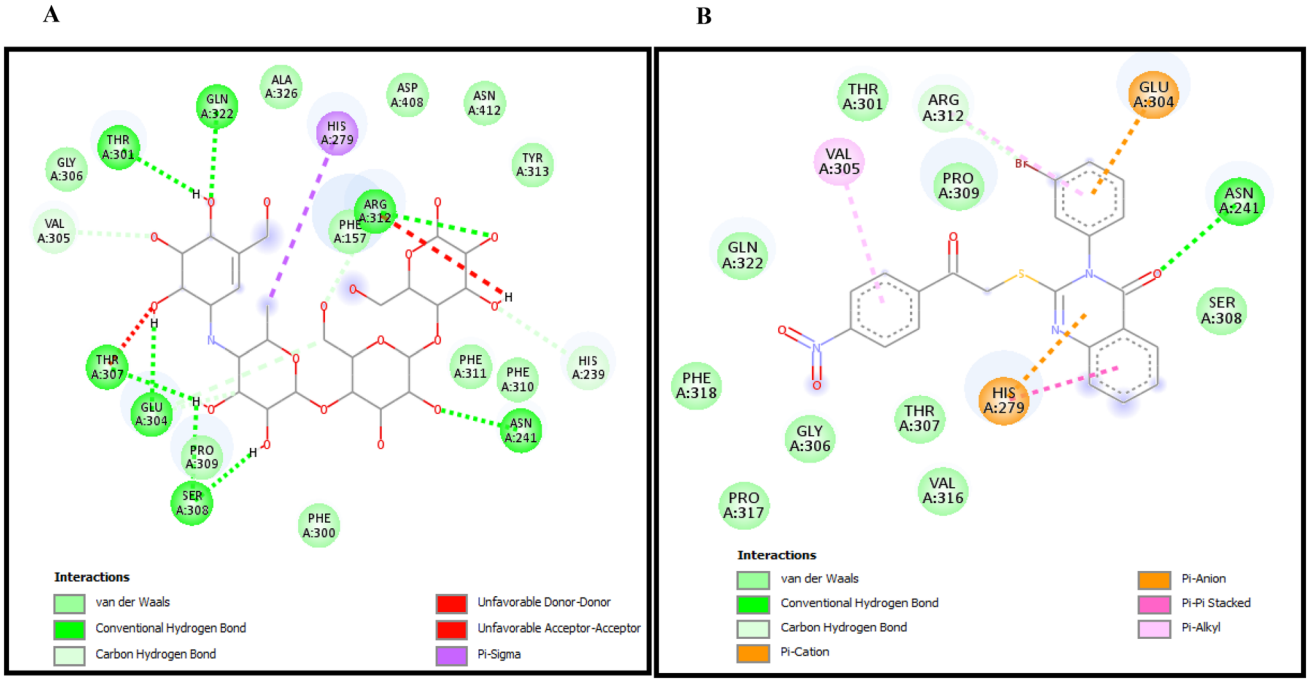

Fig. 8 **a** Interaction mode of acarbose. **b** Most potent compound **13** in the active site pocket

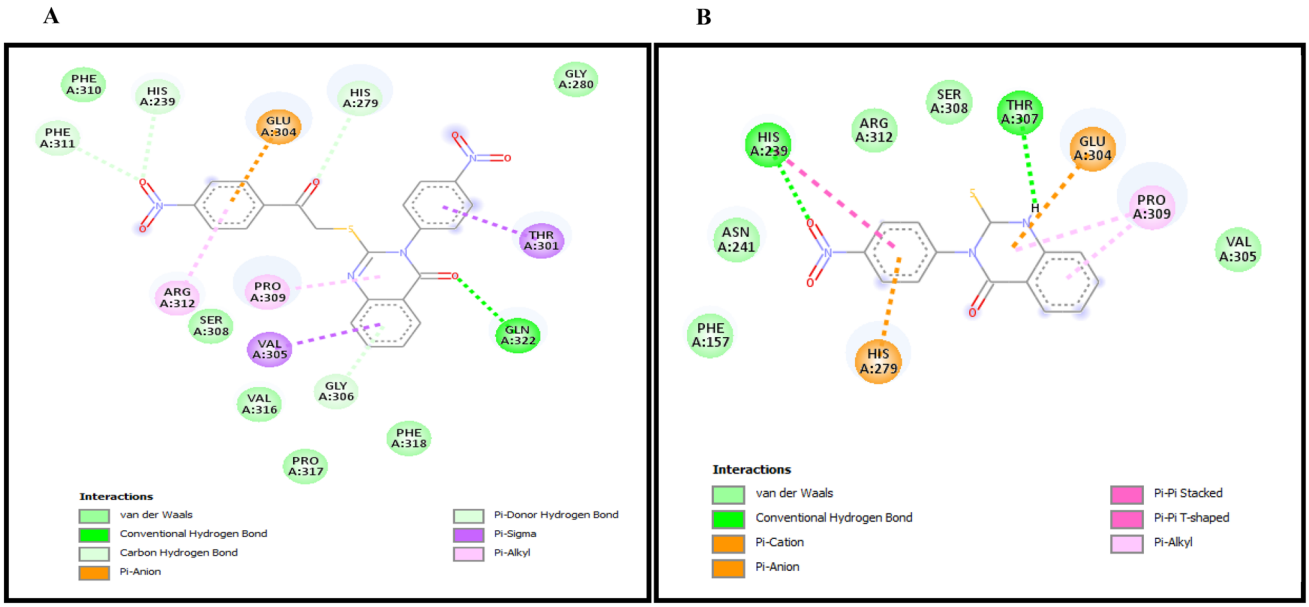

Fig. 9 **a** Interaction mode of the second potent compound **18**. **b** Compound **6** in the active site pocket

Future perspective

Our future plan is to incorporate important heterocyclic scaffolds that were reported to potentiate the pharmacological activity of the main moiety such as thiazole, thiazine, triazine, triazole, and tetrazine in order to identify novel and potent antidiabetic agents.

Experimental

Materials and methods

Chemicals and reagents were purchased from Sigma-Aldrich, USA. Thin layer chromatography was performed on pre-coated silica gel aluminum plates (GF-25, Merck, Germany). Ultraviolet light of 254 and 365 nm wavelengths was used to visualize the chromatograms. ^{1}H- and ^{13}C-NMR experiments were performed on Bruker 300, 400, and 500 MHz NMR spectrometers. Mass spectra were recorded on JEOL JMS 600H and Finnigan MAT-311A mass spectrometers. Melting points were noted on Stuart® SMP10 apparatus and are uncorrected.

General synthetic procedure for the synthesis of compounds (1–8)

Phenyl isothiocyanate derivative (1 mmol) and anthranilic acid (1 mmol) were added in absolute ethanol (10 ml) into a 100-ml round-bottomed flask. Few drops of triethylamine were added in the reaction mixture and refluxed for 2–3 h. Reaction progress was checked periodically by TLC analysis. On completion, precipitates were appeared in the reaction flask which were collected via filtration and washed with distilled water and then hexane to remove trace impurities. Crude products were crystallized from ethanol to obtained purified products.

General synthetic procedure for the synthesis of compounds (8–30)

Quinazolinone derivative (1 mmol) and phenacyl bromide derivative (1 mmol) were taken in ethanol (10 ml) into a 100-ml round-bottomed flask. Few drops of triethylamine were added and refluxed for 2 h. Product formation was monitored by TLC analysis. Product appeared in the form of precipitates which were filtered, washed with distilled water and then hexane, dried in vacuo, and crystallized from ethanol to get purified product.

3-Phenyl-2-thioxo-2,3-dihydroquinazolin-4(1*H*)-one (1) [43]

White solid; Yield: 89%; M.P.: 290–292 °C; $R_f = 0.73$ (70% EtOAc/Hexane); ^{1}H-NMR (300 MHz, DMSO-d_6): δ_H 13.01 (s, 1H, NH), 7.96 (dd, $J_{5,6} = 7.8$ Hz, $J_{5,7} = 1.2$ Hz, 1H, H-5), 7.80 (dt, $J_{7(6,8)} = 8.4$ Hz, $J_{7,5} = 1.5$ Hz, 1H, H-7), 7.49 (ovp, 4H, H-8, H-3′, H-4′, H-5′), 7.36 (t, $J_{6,5} = 8.1$ Hz, $J_{6,7} = 6.9$ Hz, 1H, H-6), 7.27 (d, $J_{2',3'} = J_{6',5'} = 6.9$ Hz, 2H, H-2′, H-6′); EI-MS: *m/z* (rel. abundance%) = 254 $[M]^+$ (66), 253 (100), 119 (21), 90 (15).

3-(2-Methoxyphenyl)-2-thioxo-2,3-dihydroquinazolin-4(1*H*)-one (2) [44]

White solid; Yield: 79%; M.P.: 255–257 °C; R_f = 0.70 (70% EtOAc/Hexane); ^{1}H-NMR (300 MHz, DMSO-d_6): δ_H 13.01 (s, 1H, NH), 7.95 (dd, $J_{5,7}$ = 1.2 Hz, $J_{5,6}$ = 9.0 Hz, 1H, H-5), 7.81 (dt, $J_{7(6,8)}$ = 9.0 Hz, $J_{7,5}$ = 3.0 Hz, 1H, H-7), 7.45 (ovp, 3H, H-6, H-8, H-6′), 7.22 (ovp, 2H, H-4′, H-3′), 7.05 (t, $J_{5'(4',6')}$ = 9.0 Hz, 1H, H-5′); EI-MS: *m/z* (rel. abundance%) = 284[M]$^+$ (10), 253 (100), 236 (17), 254 (16), 221 (15).

3-(4-Methoxyphenyl)-2-thioxo-2,3-dihydroquinazolin-4(1*H*)-one (3) [43]

White solid; Yield; 70%; M.P.: 240–242 °C; R_f = 0.66 (70% EtOAc/Hexane); ^{1}H-NMR (300 MHz, DMSO-d_6): δ_H 12.97 (s, 1H, NH), 7.94 (d, $J_{5,6}$ = 7.2 Hz, 1H, H-5), 7.78 (t, $J_{7,6}$ = 7.2 Hz, $J_{7,8}$ = 8.1 Hz, 1H, H-7), 7.44 (d, $J_{8,7}$ = 8.4 Hz, 1H, H-8), 7.35 (t, $J_{6,7}$ = $J_{6,5}$ = 7.5 Hz, 1H, H-6), 7.17 (d, $J_{2',3'}$ = $J_{6',5'}$ = 8.7, 2H, H-2′, H-6′), 7.00 (d, $J_{3',2'}$ = $J_{5',6'}$ = 8.7, 2H, H-3′, H-5′), 3.80 (s, 3H, OCH_3); EI-MS: *m/z* (rel. abundance%) = 284 [M]$^+$ (100), 283 (94), 252 (13), 162 (30).

3-(4-Ethoxyphenyl)-2-thioxo-2,3-dihydroquinazolin-4(1*H*)-one (4) [44]

White solid; Yield: 70%; M.P.: 296–297 °C; R_f = 0.69 (70% EtOAc/Hexane); ^{1}H-NMR (300 MHz, DMSO-d_6): δ_H 12.95 (s, 1H, NH), 7.94 (dd, $J_{5,7}$ = 1.2 Hz, $J_{5,6}$ = 7.8 Hz, 1H, H-5), 7.78 (dt, $J_{7,5}$ = 1.5 Hz, $J_{7,6}$ = $J_{7,8}$ = 7.8 Hz, 1H, H-7), 7.43 (d, $J_{8,7}$ = 8.1 Hz, 1H, H-8), 7.32 (dt, $J_{6(5,7)}$ = 7.8 Hz, $J_{6,8}$ = 0.6 Hz, 1H, H-6), 7.14 (d, $J_{2',3'}$ = $J_{6',5'}$ = 9.0 Hz, 2H, H-2′, H-6′), 6.97 (d, 2H, $J_{3,2}$ = $J_{5,6}$ = 8.7, H-3′, H-5′), 4.05 (q, $J_{CH2,CH3}$ = 7.2 Hz, 2H, OCH_2), 1.34 (t, 3H, $J_{CH3,CH2}$ = 6.9 Hz, CH_3); EI-MS *m/z* (rel abundance%) = 298 [M]$^+$ (100), 162 (46), 119 (19).

2-Mercapto-3-(3-nitrophenyl) quinazolin-4(3*H*)-one (5) CAS#107943-47-5

Off white solid; Yield: 68%; M.P.: 322–324 °C; R_f = 0.65 (70% EtOAc/Hexane); ^{1}H-NMR (300 MHz, DMSO-d_6): δ_H 8.34 (d, $J_{5,6}$ = 9.0 Hz, 1H, H-5), 8.20 (s, 1H, H-2′), 8.08 (d, $J_{4',5'}$ = 6.0 Hz, 1H, H-4′), 7.79 (ovp, 3H, H-6, H-5′, H-6′), 7.38 (ovp, 2H, H-7, H-8), 4.56 (s, 1H, SH); EI-MS *m/z* (rel. abundance%) = 299 [M]$^+$ (83), 298 (100), 252 (78), 267 (61), 253 (21).

3-(4-Nitrophenyl)-2-thioxo-2,3-dihydroquinazolin-4(1*H*)-one (6) [45]

Off white solid; Yield: 70%; M.P.: 316–317 °C; R_f = 0.61 (70% EtOAc/Hexane); ^{1}H-NMR (300 MHz, DMSO-d_6): δ_H 13.14 (s, 1H, NH), 8.35 (d, $J_{5',6'}$ = $J_{3',2'}$ = 10.2 Hz, 2H, H-3′, H-5′), 7.96 (d, $J_{5,6}$ = 7.8 Hz, 1H, H-5), 7.80 (t, $J_{7,6}$ = 7.2 Hz, $J_{7,8}$ = 6.9 Hz, 1H, H-7), 7.65 (d, $J_{2',3'}$ = $J_{6',5'}$ = 10.3 Hz, 2H, H-2′, H-6′), 7.45 (d, $J_{8,7}$ = 8.1 Hz, 1H, H-8), 7.36 (t, $J_{6,5}$ = 7.5 Hz, $J_{6,7}$ = 7.2 Hz, 1H, H-6); EI-MS *m/z* (rel. abundance%) = 298 [M]$^+$ (100), 299 (95), 119 (22), 252 (21).

3-(2-Fluorophenyl)-2-thioxo-2,3-dihydroquinazolin-4(1*H*)-one (7) CAS#23892-21-9

White solid; Yield: 70%; M.P.: 224–227 °C; R_f = 0.64 (70% EtOAc/Hexane); ^{1}H-NMR (300 MHz, DMSO-d_6): δ_H 13.20 (s, 1H, NH), 7.98 (d, $J_{5,6}$ = 9.0 Hz, 1H, H-5), 7.84 (dt, $J_{7(6,8)}$ = 9.0 Hz, $J_{7,5}$ = 3.0 Hz, 1H, H-7), 7.47 (ovp, 6H, H-6, H-8, H-3′, H-4′, H-5′, H-6′); EI-MS: *m/z* (rel. abundance%) = 272 [M]$^+$ (92), 253 (100), 119 (24), 163 (10).

3-(3-Chlorophenyl)-2-thioxo-2,3-dihydroquinazolin-4(1*H*)-one (8) [44]

White solid; Yield: 70%; M.P.: 231–233 °C; R_f = 0.67 (70% EtOAc/Hexane); ^{1}H-NMR (300 MHz, DMSO-d_6): δ_H 13.06 (s, 1H, NH), 7.95 (d, $J_{5,6}$ = 7.2 Hz, 1H, H-5), 7.79 (t, $J_{7(6,8)}$ = 7.2 Hz, 1H, H-7), 7.53 (ovp, 4H, H-8, H-2′, H-5′, H-6′), 7.36 (t, $J_{6,5}$ = 7.8 Hz, $J_{6,7}$ = 7.2 Hz, 1H, H-6), 7.29 (m, 1H, H-4′); EI-MS: *m/z* (rel. abundance%) = 288 [M]$^+$ (80), 290 [M + 2] (25), 287 (100), 162 (8), 119 (9).

Ethyl-2-((3-(4-ethoxyphenyl)-4-oxo-3,4-dihydroquinazolin-2-yl) thio) acetate (9) CAS#28831-42-7

White solid; Yield: 70%; M.P.: 240–243 °C; R_f = 0.51 (100% DCM); ^{1}H-NMR (300 MHz, DMSO-d_6): δ_H 8.07 (d, $J_{5,6}$ = 7.8 Hz, H-5), 7.84 (dt, $J_{7(6,8)}$ = 8.4 Hz, $J_{7,5}$ = 1.5, 1H, H-7), 7.49 (ovp, 2H, H-8, H-6), 7.35 (d, $J_{2',3'}$ = $J_{6',5'}$ = 9.0 Hz, 2H, H-2′, H-6′), 7.09 (d, $J_{3',2'}$ = $J_{5',6'}$ = 8.7 Hz, 2H, H-3′, H-5′), 4.15 (ovp, 4H, $2OCH_2$), 3.94 (s, 2H, S-CH_2), 1.39 (t, $J_{CH3,CH2}$ = 6.9 Hz, 3H, CH_3), 1.22 (t, $J_{CH3,CH2}$ = 7.2 Hz, 3H, CH_3); EI-MS: *m/z* (rel. abundance%) = 384 [M]$^+$ (100), 339 (33), 265 (70), 207 (98).

3-(2-Methoxyphenyl)-2-((2-(4-nitrophenyl)-2-oxoethyl) thio) quinazolin-4(3*H*)-one (10)

White solid; Yield: 68%; M.P.: 201–202 °C; R_f = 0.39 (100% DCM); ^{1}H-NMR (400 MHz, DMSO-d_6): δ_H 8.41 (d, $J_{3'',2''}$ = $J_{5'',6''}$ = 6.6 Hz, 2H, H-3″, H-5″), 8.31 (d, $J_{2'',3''}$ = $J_{6'',5''}$ = 6.6 Hz, 2H, H-2″, H-6″), 8.03 (dd, $J_{5,7}$ = 1.2 Hz, $J_{5,6}$ = 6.0 Hz, 1H, H-5), 7.72 (dt, $J_{7(6,8)}$ = 6.3 Hz, $J_{7,5}$ = 1.2 Hz, 1H, H-7), 7.60 (dt, $J_{6(5,7)}$ = 6.3 Hz, $J_{6,8}$ = 1.2 Hz, 1H, H-6), 7.43 (ovp, 2H, H-8, H-4′), 7.29 (d, $J_{6',5'}$ = 5.7 Hz, 1H, H-6′), 7.16 (t, $J_{5'(4',6')}$ = 5.7 Hz, 1H, H-5′), 7.05 (d, $J_{3',4'}$ = 6.0 Hz, 1H, H-3′), 4.80 (d, $J_{Ha,Hb}$ = 12.6 Hz,

1H, S-CHa), 4.68 (d, $J_{Hb,Ha}$ = 12.6 Hz, 1H, S-CHb), 3,75 (s, 3H, OCH_3); ^{13}C-NMR (125 MHz, DMSO-d_6): δ_C 193.5, 159.9, 157.2, 155.0, 149.9, 146.9, 141.2, 135.0, 131.9, 130.5, 129.6, 129.6, 126.6, 126.1, 126.1, 125.5, 123.9, 123.9, 120.9, 119.1, 112.8, 55.9, 39.1; EI-MS: *m/z* (rel. abundance%) = 447 $[M]^+$ (15), 415 (28), 384 (100), 297 (91), 234 (63), 150 (48); HREI-MS Calcd for $C_{23}H_{17}N_3O_5S$: *m/z* = 447.0889, found: 447.0868.

3-(4-Methoxyphenyl)-2-((2-(4-nitrophenyl)-2-oxoethyl) thio) quinazolin-4(3*H*)-one (11) CAS#760195-87-7

Off white solid; Yield: 70%; M.P.: 209–212 °C; R_f = 0.43 (100% DCM); ^{1}H-NMR (400 MHz, DMSO-d_6): δ_H 8.42 (d, $J_{3'',2''} = J_{5'',6''}$ = 6.3 Hz, 2H, H-3″, H-5″), 8.31 (d, $J_{2'',3''} = J_{6'',5''}$ = 6.0 Hz, 2H, H-2″, H-6″), 8.03 (d, $J_{5,6}$ = 5.7 Hz, 1H, H-5), 7.70 (t, $J_{7(6,8)}$ = 5.7 Hz, 1H, H-7), 7.42 (ovp, 3H, H-2′, H-6′), 7.14 (d, $J_{3',2'} = J_{5',6'}$ = 6.3 Hz, 2H, H-3′, H-5′), 7.03 (d, $J_{8,7}$ = 6.0 Hz, 1H, H-8), 4.72 (s, 1H, S-CH_2), 3.85 (s, 3H, OCH_3); EI-MS: *m/z* (rel. abundance%) = 447 $[M]^+$ (30), 415 (83), 297 (92), 285 (68), 265 (100), 251 (60), 150 (45).

3-(4-Ethoxyphenyl)-2-((2-(4-nitrophenyl)-2-oxoethyl) thio) quinazolin-4(3*H*)-one (12) CAS#768287-72-5

Off white solid; Yield: 70%; M.P.: 246–249 °C; R_f = 0.45 (100% Dichloromethane); ^{1}H-NMR (400 MHz, DMSO-d_6): δ_H 8.42 (d, $J_{3'',2''} = J_{5'',6''}$ = 6.6 Hz, 2H, H-3″, H-5″), 8.31 (d, $J_{2'',3''} = J_{6'',5''}$ = 6.6 Hz, 2H, H-2″, H-6″), 8.03 (d, $J_{5,6}$ = 6.0 Hz, 1H, H-5), 7.70 (t, $J_{7(6,8)}$ = 5.7 Hz, 1H, H-7), 7.42 (t, $J_{6(5,7)}$ = 6.0 Hz, 1H, H-6), 7.37 (d, $J_{2',3'} = J_{6',5'}$ = 6.6 Hz, 2H, H-2′, H-6′), 7.11 (d, $J_{3',2'} = J_{5',6'}$ = 6.3 Hz, 2H, H-3′, H-5′), 7.02 (d, $J_{8,7}$ = 6.3 Hz, 1H, H-8), 4.72 (s, 2H, S-CH_2), 4.15 (q, $J_{CH2,CH3}$ = 6.8 Hz, 2H, OCH_2), 1.39 (t, $J_{CH3,CH2}$ = 5.4 Hz, 3H, CH_3); EI-MS: *m/z* (rel. abundance%) = 461 $[M]^+$ (33), 429 (93), 400 (27), 298 (64), 279 (84).

3-(3-Bromophenyl)-2-((2-(4-nitrophenyl)-2-oxoethyl) thio) quinazolin-4(3*H*)-one (13)

White solid; Yield: 75%; M.P.: 226–228 °C; R_f = 0.34 (100% DCM); ^{1}H-NMR (400 MHz, DMSO-d_6): δ_H 8.42 (d, $J_{3'',2''} = J_{5'',6''}$ = 6.9 Hz, 2H, H-3″, H-5″), 8.31 (d, $J_{2'',3''} = J_{6'',5''}$ = 6.6 Hz. 2H, H-2″, H-6″), 8.04 (dd, $J_{5,6}$ = 5.7 Hz, $J_{5,7}$ = 1.0 Hz, 1H, H-5), 7.85 (ovp, 2H, H-8, H-6′), 7.72 (dt, $J_{7(6,8)}$ = 6.3 Hz, $J_{7,5}$ = 1.2 Hz, 1H, H-7), 7.60 (ovp, 2H, H-4′, H-5′), 7.44 (t, $J_{6,7}$ = 6.3 Hz, 1H, H-6), 7.04 (d, $J_{6',5'}$ = 6.0 Hz, 1H, H-6′), 4.76 (s, 2H, S-CH_2); ^{13}C-NMR (125 MHz, DMSO-d_6): δ_C 193.3, 160.4, 156.0, 150.0, 146.8, 141.2, 137.3, 135.0, 133.1, 132.3, 131.4, 129.6, 129.6, 128.8, 126.6, 126.1, 125.5, 123.9, 123.9, 121.7, 119.4, 39.9; EI-MS: *m/z* (rel. abundance%) = 495 $[M]^+$ (30), 497 [M + 2] (32), 464 (36), 347 (100), 333 (61), 234 (65), 150 (53); HREI-MS Calcd for $C_{23}H_{14}ClF_3N_2O_2S$: *m/z* = 494.9888, found: 494.9879.

3-(2,3-Dichlorophenyl)-2-((2-(4-nitrophenyl)-2-oxoethyl) thio) quinazolin-4(3*H*)-one (14)

White solid; Yield: 53%; M.P.: 211–214 °C; R_f = 0.29 (100% DCM); ^{1}H-NMR (300 MHz, DMSO-d_6): δ_H 8.39 (d, $J_{3'',2''} = J_{5'',6''}$ = 8.8 Hz, 2H, H-3″, H-5″), 8.29 (d, $J_{2'',3''} = J_{6'',5''}$ = 8.8 Hz, 2H, H-2″, H-6″), 8.04 (d, $J_{5,6}$ = 7.6 Hz, 1H, H-5), 7.92 (d, $J_{4',5'}$ = 8.0 Hz, 1H, H-4′), 7.75 (ovp, 2H, H-6, H-6′), 7.64 (t, $J_{7(6,8)}$ = 8.4 Hz, 1H, H-7), 7.45 (t, $J_{5'(4',6')}$ = 7.6 Hz, 1H, H-5′), 7.08 (d, $J_{8,7}$ = 8.4 Hz. 1H, H-8), 4.84 (d, $J_{Ha,Hb}$ = 16.8 Hz, 1H, S-CHa), 4.77 (d, $J_{Hb,Ha}$ = 16.8 Hz, 1H, S-CHb); ^{13}C-NMR (125 MHz, DMSO-d_6): δ_C 193.0, 159.6, 155.5, 150.0, 146.8, 141.1, 137.2, 135.5, 132.8, 132.6, 131.2, 130.6, 129.7, 129.7, 129.3, 126.7, 126.5, 125.7, 123.9. 123.9, 118.9, 39.2; EI-MS: *m/z* (rel. abundance%) = 485 $[M]^+$ (9), 487 [M + 2] (6), 489 [M + 4] (2), 450 (100), 452 (41) 418 (13), 335 (36), 287 (35), 150 (37); HREI-MS Calcd for $C_{23}H_{14}ClF_3N_2O_2S$: *m/z* = 485.0004, found: 484.9983.

3-(2-Chlorophenyl)-2-((2-(4-nitrophenyl)-2-oxoethyl) thio) quinazolin-4(3*H*)-one (15)

Yellow solid; Yield: 70%; M.P.: 187–189 °C; R_f = 0.31 (100% DCM); ^{1}H-NMR (400 MHz, DMSO-d_6): δ_H 8.41 (d, $J_{3'',2''} = J_{5'',6''}$ = 9.2 Hz, 2H, H-3″, H-5″), 8.32 (d, $J_{2'',3''} = J_{6'',5''}$ = 8.8 Hz, 2H, H-2″, H-6″), 8.06 (d, $J_{5,6}$ = 8 Hz, $J_{5,7}$ = 1.2 Hz, 1H, H-5), 7.79 (ovp, 5H, H-7, H-3′, H-4′, H-5′, H-6′), 7.46 (t, $J_{6(5,7)}$ = 7.2 Hz, 1H, H-6), 7.10 (d, $J_{8,7}$ = 8.0 Hz, 1H, H-8), 4.85 (d, $J_{Ha,Hb}$ = 16.8 Hz, 1H, S-CHa), 4.76 (d, $J_{Hb,Ha}$ = 16.8 Hz, 1H, S-CHb); ^{13}C-NMR (125 MHz, DMSO-d_6): δ_C 193.2, 159.7, 155.9, 149.9, 146.8, 141.1, 135.3, 133.1, 132.4, 132.2, 131.6, 130.3, 129.7, 129.7, 128.7, 126.7, 126.3, 125.6, 123.9, 123.9, 118.9, 39.2; EI-MS: *m/z* (rel. abundance%) = 451 $[M]^+$ (10), 453 [M + 2] (4), 416 (100), 384 (46), 301 (37), 253 (14), 234 (35), 150 (31); HREI-MS Calcd for $C_{22}H_{14}ClN_3O_4S$: *m/z* = 451.0394, found: 451.0384.

2-((2-(4-Nitrophenyl)-2-oxoethyl) thio)-3-(3-(trifluoromethyl) phenyl) quinazolin-4(3*H*)-one (16)

Off white solid; Yield: 70%; M.P.: 210–212 °C; R_f = 0.42 (100% DCM); ^{1}H-NMR (400 MHz, DMSO-d_6): δ_H 8.42 (d, $J_{3'',2''} = J_{5'',6''}$ = 8.8 Hz, 2H, H-3″, H-5″), 8.31 (d, $J_{2'',3''} = J_{6'',5''}$ = 8.8 Hz, 2H, H-2″, H-6″), 8.04 (ovp, 3H, H-5, H-2′, H-4′), 7.87 (ovp, 2H, H-5′, H-6′), 7.73 (dt, $J_{7(6,8)}$ = 8.4 Hz, $J_{7,5}$ = 1.2 Hz, 1H, H-7), 7.45 (dt, $J_{6(5,7)}$ = 8.0 Hz, $J_{6,8}$ = 0.8 Hz, 1H, H-6), 7.06 (d, $J_{8,7}$ = 8.0 Hz,

H-8), 4.82 (d, $J_{Ha,Hb}$ = 16.8 Hz, 1H, S-CHa), 4.76 (d, $J_{Hb,Ha}$ = 16.8 Hz, 1H, S-CHb); ^{13}C-NMR (125 MHz, DMSO-d_6): δ_C 193.2, 160.5, 155.8, 150.0, 146.8, 141.1, 136.7, 135.0, 133.9, 130.9, 130.4, 130.1, 129.6, 129.6, 126.9, 126.7, 126.6, 126.1, 125.5, 123.9, 123.9, 119.4, 39.5; EI-MS: *m/z* (rel. abundance%) = 485 $[M]^+$ (41), 452 (28), 335 (100), 323 (19), 289 (28), 150 (36); HREI-MS Calcd for $C_{23}H_{14}ClF_3N_3O_4S$: *m/z* = 485.0657, found: 485.0670.

2-((2-(4-Nitrophenyl)-2-oxoethyl) thio-3-(4-(trifluoromethyl) phenyl quinazolin-4(3*H*)-one (17)

White solid; Yield: 70%; M.P.: 208–209 °C; R_f = 0.38 (100% DCM); ^{1}H-NMR (400 MHz, DMSO-d_6): δ_H 8.42 (d, $J_{3'',2''} = J_{5'',6''}$ = 8.8 Hz, 2H, H-3″, H-5″), 8.31 (d, $J_{2'',3''} = J_{6'',5''}$ = 8.8 Hz, 2H, H-2″, H-6″), 8.05 (ovp, 3H, H-5, H-3′, H-5′), 7.81 (d, $J_{2',3'} = J_{6',5'}$ = 8.0 Hz, 2H, H-2′, H-6′), 7.74 (dt, $J_{7(6,\ 8)}$ = 8.4 Hz, $J_{7,5}$ = 1.2 Hz, H-7), 7.45 (t, $J_{6(5,7)}$ = 7.2 Hz, 1H, H-6), 7.06 (d, $J_{8,7}$ = 8.0 Hz, 1H, H-8), 4.77 (s, 2H, S-CH_2); ^{13}C-NMR (125 MHz, DMSO-d_6): δ_C 193.2, 160.4, 155.6, 150.0, 146.8, 141.1, 139.6, 135.1, 132.1, 130.7, 130.7, 130.3, 130.3, 129.6, 129.6, 126.8, 126.6, 126.2, 125.5, 123.9, 123.9, 119.3, 39.7; EI-MS: *m/z* (rel. abundance%) = 485 $[M]^+$ (51), 452 (30), 335 (100), 321 (27), 303 (28), 289 (31), 150 (57), 119 (15); HREI-MS Calcd for $C_{23}H_{14}F_3N_3O_4S$: *m/z* = 485.0657, found: 485.0669.

3-(4-Nitrophenyl)-2-((2-(4-nitrophenyl)-2-oxoethyl) thioquinazolin-4(3*H*)-one (18)

White solid; Yield: 69%; M.P.: 210–212 °C; R_f = 0.26 (100% DCM); ^{1}H-NMR (400 MHz, DMSO-d_6): δ_H 8.47 (ovp, 4H, H-2, H-3, H-5, H-6), 8.32 (d, $J_{3',2'} = J_{5',6'}$ = 8.8 Hz, 2H, H-3′, H-5′), 8.05 (d, $J_{5,\ 6}$ = 7.6 Hz, 1H, H-5), 7.89 (d, $J_{2',3'} = J_{6',5'}$ = 8.8 Hz, 2H, H-2′, H-6′), 7.74 (t, $J_{7(6,8)}$ = 8.0 Hz, 1H, H-7), 7.46 (t, $J_{6(5,7)}$ = 7.6 Hz, 1H, H-6), 7.08 (d, $J_{8,7}$ = 8.0 Hz, 1H, H-8), 4.80 (s, 2H, S-CH_2); ^{13}C-NMR (125 MHz, DMSO-d_6): δ_C 193.1, 160.4, 155.2, 150.0, 148.3, 146.8, 141.5, 141.1, 135.1, 131.3, 131.3, 129.6, 129.6, 126.6, 126.3, 125.6, 124.8, 124.8, 123.9, 123.9, 119.3, 39.5; EI-MS: *m/z* (rel. abundance%) = 462 $[M]^+$ (2), 430 (16), 298 (92), 252 (20), 178 (46), 150 (100), 119 (48); HREI-MS Calcd for $C_{23}H_{14}ClF_3N_2O_2S$: *m/z* = 462.0634, found: 462.0620.

3-(3-Nitrophenyl)-2-((2-(4-nitrophenyl)-2-oxoethyl) thio) quinazolin-4(3*H*)-one (19)

White solid; Yield: 72%; M.P.: 224–226 °C; R_f = 0.33 (100% DCM); ^{1}H-NMR (400 MHz, DMSO-d_6): δ_H 8.57 (t, $J_{2'(4',6')}$ = 2.0 Hz, 1H, H-2′), 8.48 (dd, $J_{5,6}$ = 8.0 Hz, $J_{5,7}$ = 1.2 Hz, 1H, H-5), 8.42 (d, $J_{3'',2''} = J_{5'',6''}$ = 8.8 Hz, 2H, H-3″, H-5″), 8.32 (d, $J_{2'',3''} = J_{6'',5''}$ = 8.8 Hz, 2H, H-2″, H-6″), 8.07 (ovp, 2H, H-4′, H-6′), 7.95 (t, $J_{7,6} = J_{7,8}$ = 8.0 Hz, 1H, H-7), 7.75 (dt, $J_{6,5} = J_{6,7}$ = 8.8 Hz, $J_{6,8}$ = 1.6 Hz, 1H, H-6), 7.46 (t, $J_{5',4'} = J_{5',6'}$ = 7.4 Hz, 1H, H-5′), 7.08 ($J_{8,7}$ = 8.4 Hz, 1H, H-8), 4.84 (d, $J_{Ha,Hb}$ = 12.6 Hz, 1H, S-CHa), 4.76 (d, $J_{Hb,Ha}$ = 12.6 Hz, 1H, S-CHb); ^{13}C-NMR (125 MHz, DMSO-d_6): δ_C 194.1, 160.2, 159.3, 152.3, 148.1, 148.9, 141.5, 134.2, 133.6, 133.4, 129.9, 129.7, 129.7, 127.3, 126.7, 126.5, 123.8, 123.8, 121.4, 120.8, 119.5, 39.5; EI-MS: *m/z* (rel. abundance%) = 462 $[M]^+$ (28), 429 (33), 312 (100), 280 (14), 266 (23), 233 (16), 150 (71); HREI-MS Calcd for $C_{22}H_{14}N_4O_6S$: *m/z* = 462.2313, found: 462.2301.

3-(4-Nitrophenyl)-2-((2-(3-nitrophenyl)-2-oxoethyl) thio) quinazolin-4(3*H*)-one (20)

White solid; Yield: 70%; M.P.: 289–290 °C; R_f = 0.35 (100% DCM); ^{1}H-NMR (400 MHz, DMSO-d_6): δ_H 8.77 (s, 1H, H-2″), 8.55 (ovp, 2H, H-4″, H-6″), 8.47 (d, $J_{3',2'} = J_{5',6'}$ = 8.8 Hz, 2H, H-3′, H-5′), 8.05 (d, $J_{5,6}$ = 7.2 Hz, 1H, H-5), 7.93 (ovp, 3H, H-2′, H-6′, H-5″), 7.73 (t, $J_{7(6,8)}$ = 7.2 Hz, 1H, H-7), 7.46 (t, $J_{6(5,7)}$ = 7.6 Hz, 1H, H-6), 7.08 (d, $J_{8,7}$ = 8.0 Hz, 1H, H-8), 4.83 (s, 2H, S-CH_2); ^{13}C-NMR (125 MHz, DMSO-d_6): δ_C 192.6, 160.4, 155.3, 148.3, 148.0, 146.8, 141.5, 137.6, 135.1, 134.5, 131.3, 131.3, 130.7, 127.7, 126.6, 126.2, 125.5, 124.8, 124.8, 122.6, 119.4, 39.2; EI-MS: *m/z* (rel. abundance%) = 462 $[M]^+$ (8), 430 (42), 401 (19), 312 (36), 298 (54), 280 (26), 150 (100), 119 (23); HREI-MS Calcd for $C_{23}H_{14}ClF_3N_2O_2S$: *m/z* = 462.0634, found: 462.0620.

3-(2-Chlorophenyl)-2-((2-(3-nitrophenyl)-2-oxoethyl) thio) quinazolin-4(3*H*)-one (21)

Off white solid; Yield: 68%; M.P.: 174–176 °C; R_f = 0.37 (100% DCM); ^{1}H-NMR (400 MHz, DMSO-d_6): δ_H 8.77 (s, 1H, H-2″), 8.54 (ovp, 2H, H-4″, H-6″), 8.06 (d, $J_{5,6}$ = 8.0 Hz, 1H, H-5), 7.92 (t, $J_{5''(4'',6'')}$ = 8.0 Hz, 1H, H-5″), 7.79 (ovp, 3H, H-7, H-3′, H-6′), 7.68 (ovp, 2H, H-5′, H-4′), 7.46 (t, $J_{6(5,7)}$ = 8.0 Hz, 1H, H-6), 7.11 (d, $J_{8,7}$ = 8.0 Hz, H-8); ^{13}C-NMR (125 MHz, DMSO-d_6): δ_C 192.7, 159.7, 155.9, 148.0, 146.8, 137.6, 135.3, 134.5, 133.1, 132.4, 132.2, 131.6, 130.6, 130.3, 128.7, 127.6, 126.7, 126.3, 125.6, 122.6, 118.9, 38.8; EI-MS: *m/z* (rel. abundance%) = 451 $[M]^+$ (17), 453 [M + 2] (6), 384 (57), 301(78), 253 (70), 150 (96), 132 (33); HREI-MS Calcd for $C_{22}H_{14}ClN_3O_4S$: *m/z* = 451.0394, found: 451.0385.

3-(4-Ethoxyphenyl)-2-((2-(3-nitrophenyl)-2-oxoethyl) thio) quinazolin-4(3*H*)-one (22) CAS#767994-98-9

White solid; Yield: 70%; M.P.: 179.0–182.5 °C; R_f = 0.46 (100% DCM); ^{1}H-NMR (400 MHz, DMSO-d_6): δ_H 8.77 (s,

1H, H-2″), 8,54 (m, 2H, H-4″, H-6″), 8.03 (d, $J_{5,6}$ = 7.6 Hz, 1H, H-5), 7.92 (t, $J_{5(4,6)}$ = 8.0 Hz, 1H, H-5″), 7.70 (dt, $J_{7(5,8)}$ = 8.4 Hz, $J_{7,5}$ = 1.2 Hz, 1H, H-7), 7.42 (ovp, 3H, H-6, H-2′, H-6′), 7.11 (d, $J_{3',2'}$ = $J_{5',6'}$ = 8.8 Hz, 2H, H-3′, H-5′), 7.02 (d, $J_{8,7}$ = 8.0 Hz, 1H, H-8), 4.75 (s, 2H, CH_2), 4.15 (quartet, $J_{CH2,CH3}$ = 7.2 Hz, 2H, OCH_2), 1.39 (t, $J_{CH3,CH2}$ = 6.8 Hz, 3H, CH_3); EI-MS: *m/z* (rel. abundance%) = 461 $[M]^+$ (37), 429 (41), 311 (100), 299 (44), 284 (30), 279 (38), 265 (24), 150 (31), 119 (16).

2-((2-(3-Nitrophenyl)-2-oxoethyl) thio)-3-(2-(trifluoromethyl) phenyl) quinazolin-4(3*H*)-one (23)

Off white solid; Yield: 60%; M.P.: 189–191 °C; R_f = 0.44 (100% DCM); ^{1}H-NMR (400 MHz, DMSO-d_6): δ_H 8.77 (t, $J_{2''(6'',4'')}$ = 2.0 Hz, 1H, H-2″), 8.54 (ovp, 2H, H-4″, H-6″), 8.05 (ovp, 6H, H-5, H-3′, H-4′, H-5′, H-6′, H-5″), 7.75 (dt, $J_{7(6,8)}$ = 8.4 Hz, $J_{7,5}$ = 1.6 Hz, 1H, H-7), 7.46 (dt, $J_{6(5,7)}$ = 8.0 Hz, $J_{6,8}$ = 0.8 Hz, 1H, H-6), 7.11 (d, $J_{8,7}$ = 8.0 Hz, 1H, H-8), 4.86 (d, $J_{Ha,Hb}$ = 16.4 Hz, 1H, S-CHa), 4.80 (d, $J_{Hb,Ha}$ = 16.8 Hz, 1H, S-Hb); ^{13}C-NMR (125 MHz, DMSO-d_6): δ_C 192.6, 160.5, 156.1, 147.9, 146.7, 137.6, 135.3, 134.5, 134.3, 133.0, 132.5, 131.4, 130.6, 127.8, 127.6, 127.3, 127.0, 126.6, 126.4, 125.6, 122.6, 118.9, 39.1; EI-MS: *m/z* (rel. abundance%) = 485 $[M]^+$ (36), 452 (34), 335 (100), 289 (18), 253 (17), 150 (26); HREI-MS Calcd for $C_{23}H_{14}F_3N_3O_4S$: *m/z* = 485.0657, found: 485.0632.

3-(3-Bromophenyl)-2-((2-(4-chlorophenyl)-2-oxoethyl) thio) quinazolin-4(3*H*)-one (24)

White solid; Yield: 75%; M.P.: 204–206 °C; R_f = 0.36 (100% DCM); ^{1}H-NMR (400 MHz, DMSO-d_6): δ_H 8.10 (d, $J_{2'',3''}$ = $J_{6'',5''}$ = 6.8 Hz, 2H, H-2″, H-6″), 8.04 (dd, $J_{5,6}$ = 8.0 Hz, $J_{5,7}$ = 1.2 Hz, 1H, H-5), 7.84 (t, $J_{2',6'}$ = $J_{2',4'}$ = 2.0 Hz, 1H, H-2′), 7.82 (m, 1H, H-4′), 7.74 (dt, $J_{7(6,8)}$ = 7.2 Hz, $J_{7,5}$ = 1.6 Hz, 1H, H-7), 7.68 (d, $J_{3'',2''}$ = $J_{5'',6''}$ = 8.8 Hz, 2H, H-3″, H-5″), 7.59 (ovp, 2H, H-6′, H-5′), 7.44 (dt, $J_{6(5,7)}$ = 8.0 Hz, $J_{6,8}$ = 1.2 Hz, 1H, H-6), 7.11 (d, $J_{8,7}$ = 8.0 Hz, 1H, H-8), 4.73 (s, 1H, S-CH_2); ^{13}C-NMR (125 MHz, DMSO-d_6): δ_C 192.8, 160.5, 156.0, 146.8, 138.4, 137.3, 135.0, 134.9, 133.0, 132.3, 131.4, 130.2, 130.2, 128.9, 128.9, 128.8, 126.6, 126.1, 125.5, 121.7, 119.4, 38.9; EI-MS: *m/z* (rel. abundance%) = 484 $[M]^+$ (11), 486 [M + 2] (16), 488 [M + 4] (4), 405 (17), 345 (32), 168 (13), 139 (100); HREI-MS Calcd for $C_{22}H_{14}BrClN_2O_2S$: *m/z* = 483.9648, found: 483.9641.

2-((2-(4-Chlorophenyl)-2-oxoethyl) thio)-3-(4-(trifluoromethyl) phenyl) quinazolin-4(3*H*)-one (25)

White solid; Yield: 85%; M.P.: 221–222 °C; R_f = 0.41 (100% DCM); ^{1}H-NMR (300 MHz, DMSO-d_6): δ_H 8.11 (d, $J_{2'',3''}$ = $J_{6'',5''}$ = 8.8 Hz, 2H, H-2″, H-6″), 8.05 (d, $J_{5,6}$ = 6.8 Hz, 1H, H-5), 8.02 (d, $J_{3'',2''}$ = $J_{5'',6''}$ = 8.4 Hz, 2H, H-3″, H-5″), 7.80 (d, $J_{3',2'}$ = $J_{5',6'}$ = 8.4 Hz, 2H, H-3′, H-5′), 7.76 (dt, $J_{7(6,8)}$ = 8.4 Hz, $J_{7,5}$ = 1.2 Hz, 1H, H-7), 7.68 (d, $J_{2',3'}$ = $J_{6',5'}$ = 8.4 Hz, 2H, H-2′, H-6′), 7.45 (t, $J_{6(5,7)}$ = 7.6 Hz, 1H, H-6), 7.12 (d, $J_{8,7}$ = 8.0 Hz, 1H, H-8), 4.73 (s, 2H, S-CH_2); ^{13}C-NMR (125 MHz, DMSO-d_6): δ_C 192.6, 160.4, 155.7, 146.8, 139.6, 138.3, 135.0, 135.0, 130.6, 130.6, 130.4, 130.4, 130.1, 130.1, 128.9, 128.9, 126.8, 126.7, 126.5, 126.1, 125.6, 119.4, 39.2; EI-MS: *m/z* (rel. abundance%) = 474 $[M^+]$ (61), 476 [M + 2] (26), 335 (82), 321 (38), 303 (31), 289 (25), 139 (100); HREI-MS Calcd for $C_{23}H_{14}ClF_3N_2O_2S$: *m/z* = 474.0417, found: 474.0406.

2-((2-(4-Chlorophenyl)-2-oxoethyl) thio)-3-(4-ethoxyphenyl) quinazolin-4(3*H*)-one (26) CAS#566902-45-2

Off white solid; Yield: 66%; M.P.: 223–225 °C; R_f = 0.47 (100% DCM); ^{1}H-NMR (300 MHz, DMSO-d_6): δ_H 8.10 (d, $J_{3'',2''}$ = $J_{5'',6''}$ = 8.4 Hz, 2H, H-3″, H-5″), 8.03 (d, $J_{5,6}$ = 8.0 Hz, 1H, H-5), 7.28 (dt, $J_{7(6,8)}$ = 8.4 Hz, $J_{7,5}$ = 1.2 Hz, 1H, H-7), 7.67 (d, $J_{2'',3''}$ = $J_{6'',5''}$ = 8.4 Hz, 2H, H-2″, H-6″), 7.42 (t, $J_{6(5,7)}$ = 8.0 Hz, 1H, H-6), 7.37 (d, $J_{2',3'}$ = $J_{6',5'}$ = 8.8 Hz, 2H, H-2′, H-6′), 7.11 (ovp, 3H, H-8, H-3′, H-5′), 4.68 (s, 2H, S-CH_2), 4.14 (q, $J_{CH2,CH3}$ = 7.2 Hz, 2H, OCH_2), 1.39 (t, $J_{CH3,CH2}$ = 6.8 Hz, 3H, CH_3); EI-MS: *m/z* (rel. abundance%) = 450 $[M^+]$ (36), 452 [M + 2] (13), 311 (100), 288 (36), 265 (28), 138 (88), 119 (22).

2-((2-Oxo-2-(*p*-tolyl) ethyl) thio)-3-(4-(trifluoromethyl) phenyl) quinazolin-4(3*H*)-one (27)

White solid; Yield: 75%; M.P.: 230–232 °C; R_f = 0.51 (100% DCM); ^{1}H-NMR (400 MHz, DMSO-d_6): δ_H 8.05 (dd, $J_{5,6}$ = 8.0 Hz, $J_{5,7}$ = 1.2 Hz, 1H, H-5), 8.03 (ovp, 4H, H-2″, H-3″, H-5″, H-6″), 7.80 (d, $J_{2,3}$ = $J_{6,5}$ = 8.4 Hz, 2H, H-2′, H-6′), 7.75 (dt, $J_{7(6,8)}$ = 8.4 Hz, $J_{7,5}$ = 1.6 Hz, 1H, H-7), 7.45 (t, $J_{6(5,7)}$ = 8.0 Hz, $J_{6,8}$ = 0.8 Hz, 1H, H-6), 7.40 (d, $J_{3'',2''}$ = $J_{5'',6''}$ = 8.0 Hz, 2H, H-3″, H-5″), 7.17 (d, $J_{8,7}$ = 8.0 Hz, 1H, H-8), 4.74 (s, 2H, S-CH_2), 2.41 (s, 3H, CH_3); ^{13}C-NMR (125 MHz, DMSO-d_6): δ_C 194.1, 160.6, 159.3, 146.9, 142.8, 136.0, 133.4, 132.4, 132.1, 129.7, 129.7, 128.8, 128.8, 128.1, 128.1, 127.3 126.7, 126.4, 125.3, 125.3, 124.2, 120.8. 38.8, 22.7; EI-MS: *m/z* (rel. abundance%) = 454 $[M^+]$ (11),

421 (19), 303 (9), 289 (6), 148 (15), 119 (100); HREI-MS Calcd for $C_{24}H_{17}N_2F_3O_2S$: *m/z* = 454.3132, found: 454.3116.

2-((2-Oxo-2-(*p*-tolyl) ethyl) thio)-3-(3-(trifluoromethyl) phenyl) quinazolin-4(3*H*)-one (28)

White solid; Yield: 62%; M.P.: 213–214 °C; R_f = 0.53 (100% DCM); ^{1}H-NMR (400 MHz, DMSO-d_6): δ_H 8.05 (d, $J_{2'',3''} = J_{6'',5''}$ = 8.0 Hz, 2H, H-2″, H-6″), 7,98 (ovp, 3H, H-5, H-2′, H-4′), 7.87 (dd, $J_{3'',2''} = J_{5'',6''}$ = 5.2 Hz, $J_{3'',5''} = J_{5'',3''}$ = 1.2 Hz, 2H, H-3″, H-5″), 7.75 (dt, $J_{7(6,8)}$ = 8.4 Hz, $J_{7,5}$ = 1.2 Hz, 1H, H-7), 7.45 (ovp, 3H, H-6, H-5′, H-6′), 7.17 (d, $J_{8,7}$ = 8.0 Hz, 1H, H-8), 4.78 (d, $J_{Ha,Hb}$ = 16.8 Hz, 1H, S-CHa), 4.72 (d, $J_{Hb,Ha}$ = 16.4 Hz, 1H, S-CHb); ^{13}C-NMR (125 MHz, DMSO-d_6): δ_C 192.9, 160.6, 156.0, 146.9, 143.9, 136.7, 134.9, 133.9, 133.7, 130.9, 130.4, 129.3, 129.3, 128.4, 128.4, 126.9, 126.7, 126.5, 126.0, 125.6, 124.7, 119.4, 39.4, 21.2; EI-MS: *m/z* (rel. abundance%) = 454 [M^+] (47), 421 (72), 321 (23), 303 (19), 289 (15), 145 (14), 119 (100); HREI-MS Calcd for $C_{24}H_{17}N_2F_3O_2S$: *m/z* = 454.0963, found: 454.0975.

3-(2,3-Dichlorophenyl)-2-((2-oxo-2-(*p*-tolyl) ethyl) thio) quinazolin-4(3*H*)-one (29)

Off white solid; Yield: 83%; M.P.: 174–177 °C; R_f = 0.49 (100% DCM); ^{1}H-NMR (300 MHz, DMSO-d_6): δ_H 8.04 (d, $J_{5,6}$ = 6.8 Hz, 1H, H-5), 7.96 (d, $J_{2'',3''} = J_{6'',5''}$ = 8.4 Hz, 2H, H-2″, H-6″), 7.91 (dd, $J_{4',2'}$ = 1.6 Hz, $J_{4',3'}$ = 8.4 Hz, 1H, H-4′), 7.76 (ovp, 2H, H-6, H-2′), 7.63 (t, $J_{7(6,8)}$ = 8.4 Hz, 1H, H-7), 7.45 (t, $J_{3(2,4)}$ = 7.2 Hz, 1H, H-3′), 7.37 (d, $J_{3'',2''} = J_{5'',6''}$ = 8.0 Hz, 2H, H-3″, H-5″), 7.18 (d, $J_{8,7}$ = 8.0 Hz, 1H, H-8), 4.79 (d, $J_{Ha,Hb}$ = 16.8 Hz, 1H, S-CHa), 4.73 (d, $J_{Hb,Ha}$ = 16.4 Hz, 1H, S-CHb); ^{13}C-NMR (125 MHz, DMSO-d_6): δ_C 192.7, 159.7, 155.6, 146.9, 143.9, 135.4, 135.1, 133.7, 132.7, 132.5, 131.2, 130.6, 129.3, 129.2, 129.2, 128.4, 128.4, 126.7, 126.4, 125.8, 118.9, 39.2, 21.2; EI-MS: *m/z* (rel. abundance%) = 454 [M^+] (7), 456 [M + 2] (6), 458 [M + 4] (3), 419 (100), 287 (18), 148 (11), 119 (90); HREI-MS Calcd for $C_{23}H_{14}Cl_2N_2O_2S$: *m/z* = 454.0184, found: 454.0199.

3-(3-Bromophenyl)-2-((2-oxo-2-(*p*-tolyl) ethyl) thio) quinazolin-4(3*H*)-one (30)

White solid; Yield: 78%; M.P.: 211–215 °C; R_f = 0.50 (100% DCM); ^{1}H-NMR (300 MHz, DMSO-d_6): δ_H 8.04 (dd, $J_{5,6}$ = 8.0 Hz, $J_{5,7}$ = 1.2 Hz, 1H, H-5), 7.98 (d, $J_{2'',3''} = J_{6'',5''}$ = 8.4 Hz, 2H, H-2″, H-6″), 7.84 (t, $J_{2'(6',4')}$ = 1.2 Hz, 1H, H-2′), 7.81 (m, 1H, H-4′), 7.74 (dt, $J_{7(6,8)}$ = 8.4 Hz, $J_{7,5}$ = 1.6 Hz, 1H, H-7), 7.59 (ovp, 2H, H-2′, H-3′), 7.44 (ovp, 3H, H-6, H-3″, H-5″), 7.16 (d, $J_{8,7}$ = 8.0 Hz, 1H, H-8), 4.77 (d, $J_{Ha,Hb}$ = 12.6 Hz, 1H, S-CHa), 4.72 (d, $J_{Hb,Ha}$ = 12.3 Hz, 1H, S-CHb), 2.40 (s, 1H, CH_3); ^{13}C-NMR (125 MHz, DMSO-d_6): δ_C 192.9, 160.5, 156.1, 146.9, 143.9, 137.3, 134.9, 133.8, 133.0, 132.3, 131.4, 129.3, 129.3, 128.8, 128.4, 128.4, 126.6, 126.0, 125.7, 121.7, 119.0, 39.0, 21.2; EI-MS: *m/z* (rel. abundance%) = 464 [M^+] (10), 466 [M + 2] (11), 431 (14), 433 (13), 385 (12), 119 (100); HREI-MS: Calcd for $C_{23}H_{17}BrN_2O_2S$: *m/z* 464.0194, found: 464.0189.

Acknowledgements The authors are thankful to the Pakistan Academy of Sciences, Pakistan, for providing financial support to Project No. (5-9/PAS/440).

References

1. S. Ibrahim, A. Al-Ahdal, A. Khedr, G. Mohamed, Rev. Bras. Farmacogn. **27**, 170 (2017)
2. J.C. Burani, L. Rao, *Good Carbs, Bad Carbs: An Indispensable Guide to Eating the Right Carbs for Losing Weight and Optimum Health*. Marlowe and Company, 2002.
3. M. Ajaib, S. Fatima, S.H. Kamran, K.M. Khan, S. Perveen, S. Shah, J. Chem. Soc. Pak. **38**, 1267 (2016)
4. M. Ajaib, M. Latif, S.H. Kamran, K.M. Khan, S. Perveen, S. Shah, A. Karim, J. Chem. Soc. Pak. **38**, 313 (2016)
5. M.A. Abbasi, S.A.H. Shah, Aziz-ur-Rehman, S.Z. Siddiqui, G. Hussain, K.M. Khan, M. Ashraf, S.A. Ejaz, J. Chem. Soc. Pak. **39**, 248 (2017).
6. H. King, M. Rewers, Diabetes Care **16**, 57 (1993)
7. P.R. Flanagan, G.G. Forstner, Biochem. J. **173**, 553 (1978)
8. S. Chiba, Bioscience, Biotechnol. Biochem. **61**, 1233 (1997)
9. K.T. Kim, L.E. Rioux, S.L. Turgeon, Phytochemistry **9**, 827 (2014)
10. A.R. Saltiel, C.R. Kahn, Nature **414**, 799 (2001)
11. H. Sun, D. Wang, X. Song, Y. Zhang, W. Ding, X. Peng, X. Zhang, Y. Li, Y. Ma, R. Wang, J. Agric Food Chem. **65**, 1574 (2017)
12. P.M. Heacock, S.R. Hertzler, J.A. Williams, B.W. Wolf, J. Am. Diet. Assoc. **105**, 65 (2005)
13. S.D. Kim, Food Chem. **136**, 297 (2013)
14. N. Jong-Anurakkun, M.R. Bhandari, J. Kawabata, Food Chem. **103**, 1319 (2007)
15. J.J. DiNicolantonio, J. Bhutani, J.H. O'Keefe, Open Heart **2**, 1 (2015)
16. M.A. Avery, C.S. Mizuno, A.G. Chittiboyina, T.W. Kurtz, H.A. Pershadsingh, Curr. Med. Chem. **15**, 61 (2008)
17. B.R. Miller, H. Nguyen, C.J.H. Hu, C. Lin, Q.T. Nguyen, Am. Health Drug Benef. **7**, 452 (2014)
18. A.D. Mooradian, J.E. Thurman, Drugs **57**, 19 (1999)
19. M.M. Wang, G.L. Dou, D.Q. Shi, J. Heterocycl. Chem. **47**, 939 (2010)
20. O.O. Ajani, Bangladesh. J. Pharmacol. **11**, 716 (2016)
21. I. Monreal, M. Sánchez-Castellanos, K. Ramírez-Gualito, G. Cuevas, K.A. Espinoza, I.A. Rivero, J. Braz. Chem. Soc. **30**, 124 (2019)
22. M. Asif, Int. J. Med. Chem. **2014**, 1 (2014)
23. S.K. Pandey, A. Singh, A. Singh, Eur. J. Med. Chem. **44**, 1188 (2009)
24. M.A. Mohamed, R.R. Ayyad, T.Z. Shawer, A.-M. Alaa, A.S. El-Azab, Eur. J. Med. Chem. **112**, 106 (2016)
25. S. Allameh, M. Heravi, M. Hashemi, F. Bamoharram, Chin. Chem. Lett. **22**, 131 (2011)
26. N.M.A. Gawad, H.H. Georgey, R.M. Youssef, N.A. El Sayed, Med. Chem. Res. **20**, 1280 (2011)

27. G. Moussa, R. Alaaeddine, L.M. Alaeddine, R. Nassra, A.S. Belal, A. Ismail, A.F. El-Yazbi, Y.S. Abdel-Ghany, A. Hazzaa, Eur. J. Med. Chem. **144**, 635 (2018)
28. F.M. Refaie, A.Y. Esmat, S.M.A. Gawad, A.M. Ibrahim, M.A. Mohamed, Lipids Health Dis. **4**, 22 (2005)
29. Y.I. El-Gazzar, H.H. Georgey, S.M. El-Messery, H.A. Ewida, G.S. Hassan, M.M. Raafat, M.A. Ewida, H.I. El-Subbagh, Bioorg. Chem. **72**, 282 (2017)
30. M. Redondo, J.G. Zarruk, P. Ceballos, D.I. Pérez, C. Pérez, A. Perez-Castillo, M.A. Moro, J. Brea, C. Val, M.I. Cadavid, Eur. J. Med. Chem. **47**, 175 (2012)
31. S.T. Al-Rashood, G.S. Hassan, S.M. El-Messery, M.N. Nagi, E.S.E. Habib, F.A. Al-Omary, H.I. El-Subbagh, Bioorg. Med. Chem. Lett. **24**, 4557 (2014)
32. G.G. Berest, O.Y. Voskoboynik, S.I. Kovalenko, O.M. Antypenko, I.S. Nosulenko, A.M. Katsev, O.S. Shandrovskaya, Eur. J. Med. Chem. **46**, 6066 (2011)
33. M.L. Heil, N.D. Cosford, R. Ardecky, and J. Zou, Google Patents, U.S. Patent No. 9,598,402. Washington, DC: U.S. Patent and Trademark Office (2017).
34. Y. Kabri, N. Azas, A. Dumetre, S. Hutter, M. Laget, P. Verhaeghe, A. Gellis, P. Vanelle, Eur. J. Med. Chem. **45**, 616 (2010)
35. H. Niaz, H. Kashtoh, J.A. Khan, A. Khan, M.T. Alam, K.M. Khan, S. Perveen, M.I. Choudhary, Eur. J. Med. Chem. **95**, 199 (2015)
36. U. Salar, M. Taha, K.M. Khan, N.H. Ismail, S. Imran, S. Perveen, S. Gul, A. Wadood, Eur. J. Med. Chem. **122**, 196 (2016)
37. K.M. Khan, F. Rahim, A. Wadood, N. Kosar, M. Taha, S. Lalani, A. Khan, M.I. Fakhri, M. Junaid, W. Rehman, Eur. J. Med. Chem. **81**, 245 (2014)
38. F. Rahim, H. Ullah, M.T. Javid, A. Wadood, M. Taha, M. Ashraf, A. Shaukat, M. Junaid, S. Hussain, W. Rehman, Bioorg. Chem. **62**, 15 (2015)
39. K. Javaid, S.M. Saad, S. Rasheed, S.T. Moin, N. Syed, I. Fatima, U. Salar, K.M. Khan, S. Perveen, M.I. Choudhary, Bioorg. Med. Chem. **23**, 7417 (2015)
40. H. Kashtoh, S. Hussain, A. Khan, S.M. Saad, J.A. Khan, K.M. Khan, S. Perveen, M.I. Choudhary, Bioorg. Med. Chem. **22**, 5454 (2014)
41. M. Taha, N.H. Ismail, S. Lalani, M.Q. Fatmi, S. Siddiqui, K.M. Khan, S. Imran, M.I. Choudhary, Eur. J. Med. Chem. **92**, 387 (2015)
42. S. Hameed, F. Seraj, R. Rafique, S. Chigurupati, A. Wadood, A.U. Rehman, V. Venugopal, U. Salar, M. Taha, K.M. Khan, Eur. J. Med. Chem. **183**, 1 (2019)
43. M. Adib, F. Peytam, M. Rahmanian-Jazi, S. Mahernia, H.R. Bijanzadeh, M. Jahani, M. Mohammadi-Khanaposhtani, S. Imanparast, M.A. Faramarzi, M. Mahdavi, Eur. J. Med. Chem. **155**, 353 (2018)
44. A.I. Khodair, M.A. Alsafi, M.S. Nafie, Carbohydr. Res. **486**, 107832 (2019)
45. W. Liu, Q. Zhang, F. Gong, Z. Cao, Y. Huo, J. Heterocycl. Chem. **52**, 317 (2015)
46. H.X. Wang, H.Y. Liu, W. Li, S. Zhang, Z. Wu, X. Li, C.-W. Li, Y.M. Liu, B.Q. Chen, Med. Chem. Res. **28**, 203 (2019)